Gravity and Seismic Investigation of a Portion of the Taku Glacier, Alaska

Warren Caldwell

Advisors

Robert Phinney

Anthony Dahlen

Submitted in partial fulfillment of the
requirements for the degree of Bachelor of Arts
Department of Geosciences

Princeton University
Princeton, New Jersey
April 2005

I hereby declare that I am the sole author of this thesis.

Warren Caldwell

Photograph 1. View west across Taku Glacier from the Camp 10 nunatak. Flags marking a part of Profile IV lead up the right side of the photograph. Figures in the lower right give scale. (Credit: Paul Illsley)

Photograph 2. The Camp 10 nunatak viewed from the Taku Glacier. The reference station FFGR19.1 used in our gravity survey was located atop this nunatak. (Credit: Paul Illsley)

Photograph 3. View south (down-glacier) from the Camp 10 nunatak toward the terminus of the Taku Glacier. (Credit: Paul Illsley)

Photograph 4. View north (up-glacier) from the Camp 10 nunatak. Figures give scale. (Credit: Paul Illsley)

TABLE OF CONTENTS

LIST OF FIGURES

ACKNOWLEDGEMENTS

I would like to thank my advisors at Princeton University, Dr. Robert Phinney and Dr. Anthony Dahlen, for all their advice and guidance in bringing this project to completion. The modeling approach used here was their concept. This project would not have taken place without Dr. William Isherwood, our mentor in the field and the source of my instruction on both field methods and reduction of gravity data. I would like to thank Dr. Maynard Miller of the University of Idaho and the Foundation for Glacial and Environmental Research for his work in establishing and running the Juneau Icefield Research Program (JIRP), under which my fieldwork took place. I would also like to extend my thanks to the instructors, the staff, and my fellow participants in JIRP 2004 for making it such a worthwhile and beneficial experience. The Department of Geosciences at Princeton University generously provided the funding for my participation in the program. The seismic data used here was provided by Dr. Kenneth Sprenke of the University of Idaho, who also instructed me on migration of reflection data. I could not have asked for a more conscientious partner during fieldwork than Aaron Mordecai of the University of Utah. Werner Stempfhuber, Martin Lang, and the rest of the 2004 JIRP survey team provided high quality data on the locations of our gravity stations. Dr. William Bonini of Princeton University lent his experience with gravimetry to advise on making terrain corrections. Dr. Gregg Lamorey and Phil Druker of JIRP also supervised and assisted in our fieldwork. I did all gravity modeling and seismic migration in MATLAB 7, with the exception of the digitization of seismic records, for which I used Surfer 7.

ABSTRACT

The Taku Glacier is the largest glacier in the Juneau Icefield, which is located in southeastern Alaska. Recent seismic reflection surveys have found the Taku to be, at 1400 m, the deepest temperate glacier on record, although previous seismic work had suggested its depth was only 350 m. During the 2004 summer field season, as a participant in the Juneau Icefield Research Program, I conducted a gravity survey in this location of the glacier in an attempt to test these findings. I created an analytical forward model of a glacial cross section in order to solve for the Bouger anomaly, and found, from two different trials, depths of 1214±89 m and 1328±93 m at the deepest point of the cross section. This confirms the most recent seismic work, and indicates that the base of the glacier is ~300 m below sea level at the cross section measured, which is 25 km up-glacier from the terminus. The success of gravity methods to generate reliable cross sections suggests that gravity surveys could play an important role in future study on the Juneau Icefield.

INTRODUCTION

The Juneau Icefield is located in southeastern Alaska, with its southern edge 10-15 km from the city of Juneau and its northern edge in northwestern British Columbia, Canada. The Icefield covers hundreds of square kilometers and is composed of several dozen separate glaciers, of which the Taku Glacier is the largest (Figure 1). The Taku is up to 6 km wide and measures approximately 50 km in length. Previous studies indicate that the Taku is the thickest and deepest temperate glacier ever measured (Nolan *et al*., 1995). The Taku flows southeast from the center of the Icefield to its terminus in the Taku River. The glacier has dammed the river in the past. The Taku is also presently one of only two glaciers on the Icefield that are in a state of advance (Miller, 2004; Nolan *et al*., 1995). The other glaciers on the Icefield, like the vast majority of North American glaciers, are retreating.

The extreme size and anomalous advance of the Taku Glacier make it a site of potential global interest. A detailed understanding of the characteristics of the glacier's flow and mass balance, including vertical and transverse velocity profiles, inputs, and discharge, will allow for a more complete analysis of the Taku's response to current and future climate conditions. This will contribute to the understanding of what determines the health of temperate glaciers, and how these glaciers respond to climate. Some of the required data for characterizing the behavior of a glacier, such as transverse velocity profiles and mass balance, are collected annually on the Icefield. Other data, such as flow rate and discharge, can be estimated using glacial flow laws (Nye, 1952, 1965), which require accurate measurements of a glacier's thickness and the shape of its bedrock interface. These data are sparse on the Icefield, and this thesis will address using gravimetric measurements to determine these two parameters.

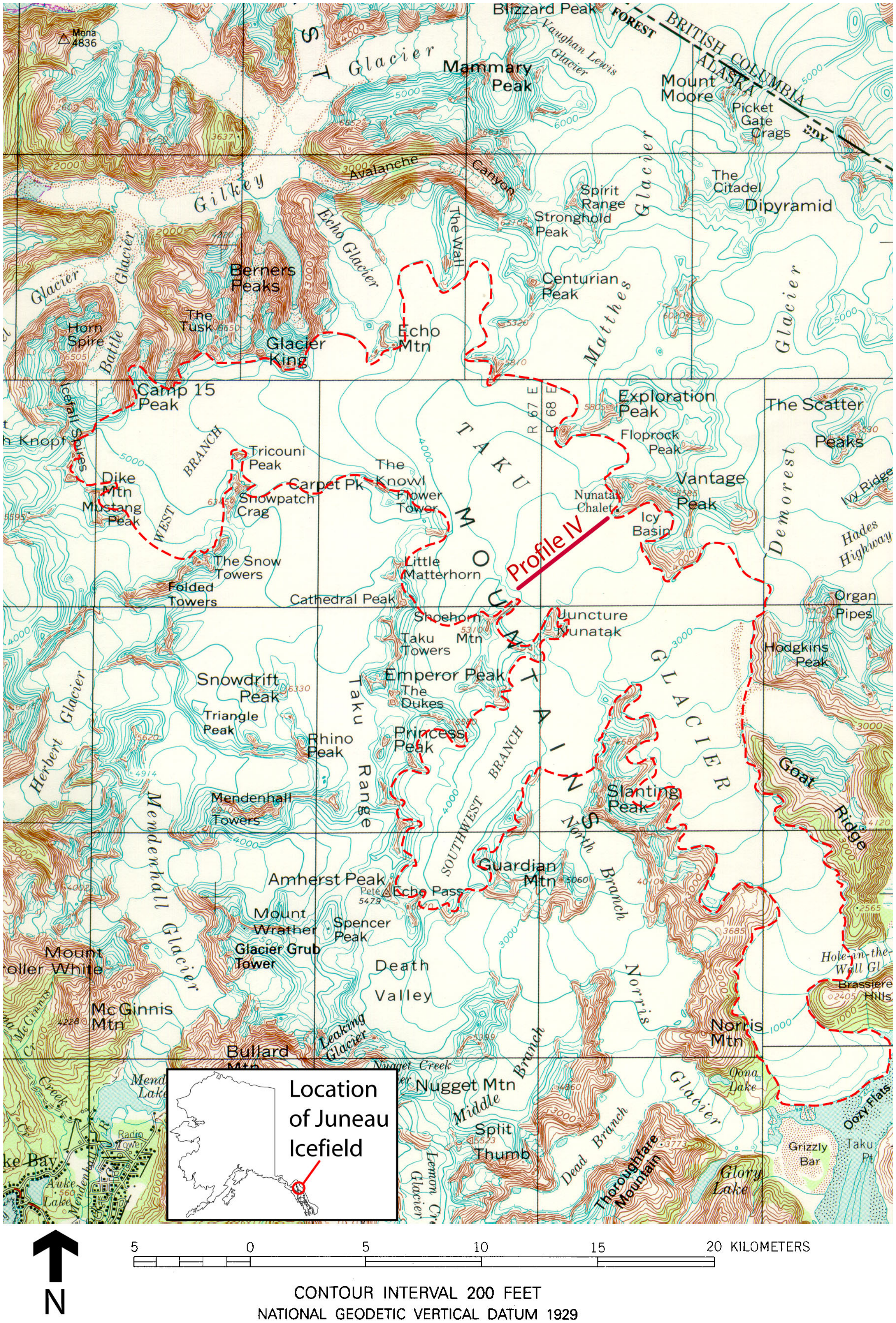
Blizzard Peak
BRITISH COLUMBIA
ALASKA
Mammary Peak
Mount Moore
Picket Gate Crags
The Citadel
Dipyramid
Spirit Range
Stronghold Peak
Avalanche
Canyon
Gilkey
Echo Glacier
The Wall
Berners Peaks
Centurian Peak
Matthes
Glacier
Horn Spire
Battle
The Tusk
Glacier King
Echo Mtn
Camp 15 Peak
Exploration Peak
The Scatter
Peaks
Floprock Peak
Icefall Spires
Knopf
Tricouni Peak
WEST BRANCH
Dike Mtn
Mustang Peak
Carpet Pk
Snowpatch Crag
The Knowl
Flower Tower
TAKU MOUNTAINS
Nunatak Chalet
Vantage Peak
Icy Basin
Demorest
Ivy Ridge
Hades Highway
Profile IV
The Snow Towers
Folded Towers
Little Matterhorn
Cathedral Peak
Organ Pipes
Shoehorn Mtn
Juncture Nunatak
Taku Towers
Hodgkins Peak
Snowdrift Peak
Emperor Peak
The Dukes
Triangle Peak
Herbert Glacier
Taku Range
Princess Peak
Rhino Peak
GLACIER
SOUTHWEST BRANCH
Goat Ridge
Mendenhall Towers
Slanting Peak
Mendenhall Glacier
North Branch
Guardian Mtn
Amherst Peak
Echo Pass
Mount Wrather
Spencer Peak
Glacier Grub Tower
Hole-in-the-Wall Gl
Brassiere Hills
Mount Troller White
Death Valley
Norris
McGinnis Mtn
Norris Mtn
Bullard Mtn
Leaking Glacier
Nugget Creek
Nugget Mtn
Middle Branch
Split Thumb
Dead Branch
Thoroughfare Mountain
Glory Lake
Grizzly Bar
Taku Pt
Oozy Flats
Auke Lake
Location of Juneau Icefield
N
5 0 5 10 15 20 KILOMETERS
CONTOUR INTERVAL 200 FEET
NATIONAL GEODETIC VERTICAL DATUM 1929

Figure 1. (Previous page) Setting of the Taku Glacier and location of the Juneau Icefield. Image taken from USGS Topographic map, 1:250000, Juneau (original scale not maintained).

The work in this thesis deals with a single transverse profile on the Taku, Profile IV, located ~30 km up-glacier from the terminus and ~5 km above the glacier's equilibrium line (Figure 1). Profile IV is of interest because it was one of the first sites on the Icefield to undergo geophysical investigation (Poulter *et al*., 1949). The results of that work, which are now believed to be in error of 400 percent (Nolan, 1992), were accepted for over 40 years. The work in this thesis will be to test the currently accepted findings using a different geophysical technique (gravity instead of seismic), and to assess the accuracy of a gravity survey on the Icefield in order to gauge the feasibility of using this method to find the ice thickness in other parts of the Icefield.

Existing geophysical work on the Taku Glacier

Less than ten well-documented geophysical investigations have been done on the Taku since 1949, some with conflicting results. Nearly all of these have relied on seismic methods. One of the first investigations of the Taku was by Poulter *et al.* (1949). Poulter had successfully conducted seismic work on ice in Antarctica, and believed it to be a more promising method than techniques like resistivity or radar. Poulter used his own 'Poulter Method,' in which the explosive charges are placed on stakes above the surface of the ice rather than buried in shot holes. This was because he believed that the reflections on the Taku would be so shallow that they would be masked by the direct arrivals if the charges were set off in shot holes. Firing the shots in the air would attenuate ground waves, decreasing their chances of masking potential reflections, and would concentrate energy in the vertical direction, strengthening reflections.

The expedition took hundreds of records on different parts of the glacier and used seventeen records on Profile IV to generate a cross section showing a uniform U-shaped valley (Figure 2). The maximum thickness of the glacier was 1144 ft (350 m). Later measurements would exceed this value by approximately 1000 m; Nolan *et al.* (1995) speculate that the waves interpreted as basal reflections were actually part of the direct wave trains, and that the seismograms did not span enough time to record the deeper, true

reflections. Attempts to replicate these results by the Poulter Method (Miller *et al*., 1993) were largely unsuccessful.

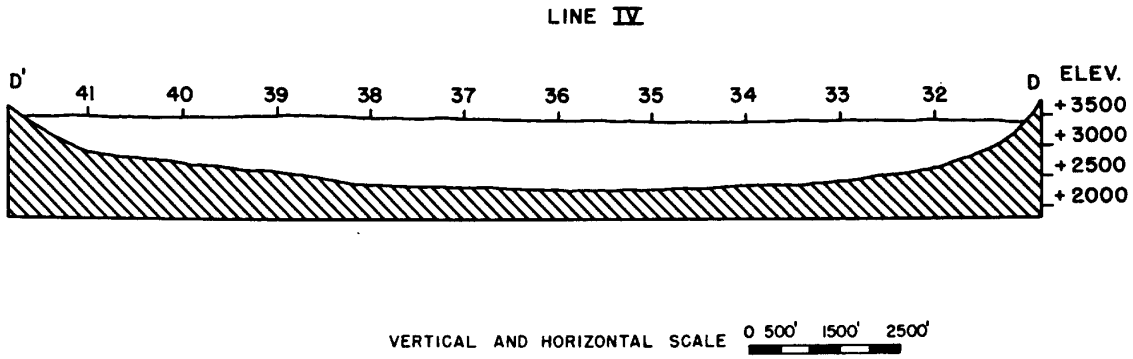

Figure 2. Cross section of Profile IV according to Poulter *et al.* (1949), now known to be incorrect.

The work of Poulter *et al*. (1949) was accepted until the 1990s; during that time, little geophysical work was done on the Taku, and there was no reinvestigation of Profile IV. A gravity survey from the intervening years (Benedict, 1984) determined the thickness of the Matthes Glacier, a tributary of the Taku, to be 586±100 m, which was an unexpected result given that this far exceeded the believed 350 m depth of the Taku. It is unlikely that a tributary could be substantially deeper than the main branch, so the author believed his result to be in error. However, given the new depth of the Taku, the findings of Benedict (1984) are most likely accurate.

The first work to directly question the results of Poulter *et al*. (1949) was conducted by Nolan (1992). Nolan pointed out that a flow law analysis of the Taku using a 350 m depth suggested that over sixty percent of the glacier's observed surface movement must come from basal slip. This implied that the Taku is a surging glacier, when in fact its movement is regular and uniform. If the glacier were deeper than 350 m, more of the observed surface movement could be accommodated by viscous flow rather than basal slip.

Nolan (1992) used six shot points and four geophone array placements across Profile IV for his reflection survey, and ultimately chose thirteen likely reflections from which to create a cross section. The reflections were picked from a hardcopy, with times and angles calculated by hand, then migrated to a spatial location. The resulting cross

section (Figure 3) was drawn by eye to match the locations of the reflectors. Nolan (1992) concluded that the Taku was at least 1400 m deep at the center of Profile IV, implying that its base was approximately 400 m below sea level.

Post-glacial rebound in southeast Alaska is substantial, so this depth may have been even greater in the past. Analysis of tide gauge data indicates uplift rates of 14 mm/yr in the vicinity of the Taku Glacier (Larsen *et al*., 2004). The authors believe that this uplift is consistent with isostatic rebound resulting from the glacial retreat of the last ~250 years.

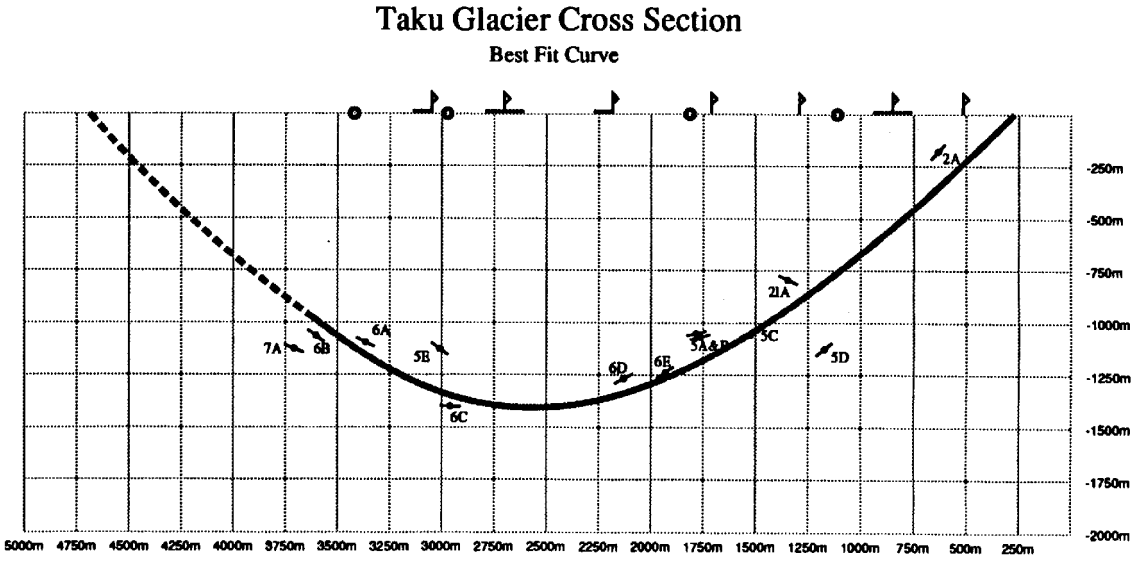

Figure 3. Cross section of Profile IV from Nolan (1992). Reflectors used to draw cross section shown.

Because the results of Nolan (1992) exceeded those of Poulter *et al*. (1949) by over 400 percent, they prompted a new round of seismic surveys in the following field seasons. Miller *et al*. (1993) conducted seismic investigations on six areas of the Icefield, including Profile IV and profiles on several other glaciers. The authors tested at least seven different combinations of source-receiver placements and shot types in order to find the method yielding the clearest results. The above-ground shot method of Poulter *et al*. (1949) was considered the most successful, since it generated clear reflections at most of the study sites – other than those on the Taku. No clear reflections were found on any Taku profile using this method.

In the following year, a more complete reflection survey was carried out on Profile IV (Sprenke *et al*., 1994) in the method of Nolan (1992). Five shot points and eight geophone array placements were used to generate the equivalent of a geophone array spanning the entire length of the profile. On three occasions, the same geophone placements were used to record shots from both the left and the right of the array. The survey yielded 33 records, which were printed out in hardcopy and the reflections picked out by hand, according to the criteria that they be continuous across several records. The calculation of the timing and slopes of the reflections, and the migration of the reflectors, was done in a spreadsheet. The final cross section agreed with the 1400 m depth found by Nolan (1992), although the number of reflectors used in plotting was far greater, so the resolution of the cross section increased accordingly. However, the shape of the cross section generated was not a typical, smooth, U-shaped glacial valley. It was somewhat V-shaped, with a plunging center (Figure 4). It also showed horizontal features at ~500-600 m elevation, which were interpreted as berm levels from a previous glaciation.

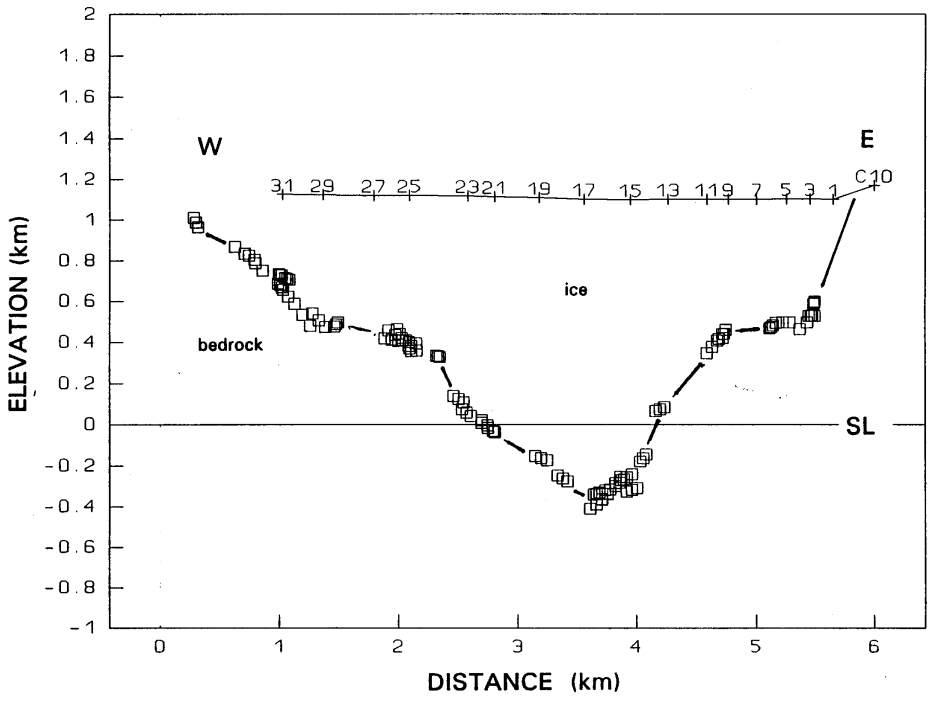

Figure 4. Cross section of Profile IV according to the seismic survey of Sprenke *et al*. (1994).

Although there is agreement between recent seismically based interpretations of ice thickness at Profile IV, a gravity survey offers a good test of these findings, since these two geophysical techniques are not subject to the same sources of error. A gravity survey indicating similar results would serve as independent confirmation of the existing interpretation. For comparison with the results of the gravity survey, I re-migrated and reanalyzed the records of Sprenke *et al.* (1994), which were the most current and complete seismic records for Profile IV.

Gravity surveys on glaciers

Glaciers are particularly well suited to gravity surveys because the density contrast between ice and bedrock is the highest of any two geologic materials, causing very large anomalies. Gravimetric measurements have been used to find ice thickness on glaciers since the 1950s (Bull and Hardy, 1956; Russell *et al*., 1960; Thiel *et al*., 1957). Most of these model the glacier as an infinite slab, although Thiel used the line integral method of Hubbert (1948).

Several gravity surveys have been conducted on the Icefield in recent years (Benedict, 1984; Venteris and Miller, 1993), but the results have generally not been as reliable as those of the seismic investigation. This can be attributed mainly to the quality of the location data and the reliability of the equipment used. Benedict (1984) estimated the locations and elevations of the observing stations from a topographic map; this dominated other sources of error and led to an uncertainty of ±18 percent in the final cross section. Additionally, the gravimeter used in these surveys may have suffered from temperature regulation problems or a damaged mechanism, or both (Miller, 2004). For the work conducted in this project, the JIRP survey team provided GPS locations of the observing stations with accuracies of several centimeters, and the gravimeter was a well-maintained and reliable unit. Combined with a more robust method of inversion, I hope to be able to generate results that are more reliable than those found in previous gravity surveys on the Icefield.

METHODS

Location

The data used in this project came from a gravity survey that I conducted with Aaron Mordecai of the University of Utah, under the supervision of Dr. William Isherwood, during the 2004 summer field season on the Juneau Icefield. Our survey was along Profile IV, a transverse line across the Taku Glacier. We sited our observing stations at points established and marked by a survey team conducting their own work on the glacier; the data that they shared with us was essential to this project. The survey team used a DGPS (differential GPS) system capable of 1-3 cm horizontal accuracy and vertical accuracy of twice this amount. As a result, we knew the locations of our observing stations with great accuracy. The survey team planted and surveyed 30 flags across Profile IV, of which we used 15 as observing stations (Figure 5). This gave a spacing of approximately 250 m between stations. We placed and surveyed an additional two stations between the easternmost survey flag and the eastern edge of the glacier, bringing the total number of observing stations to 17. On the western side of the glacier, heavy crevassing prevented either the survey team or our gravity team from approaching within ~1 km of the glacier's edge, so the 17 gravity stations span only the eastern 4.5 km of the glacier's total width of ~5.5 km.

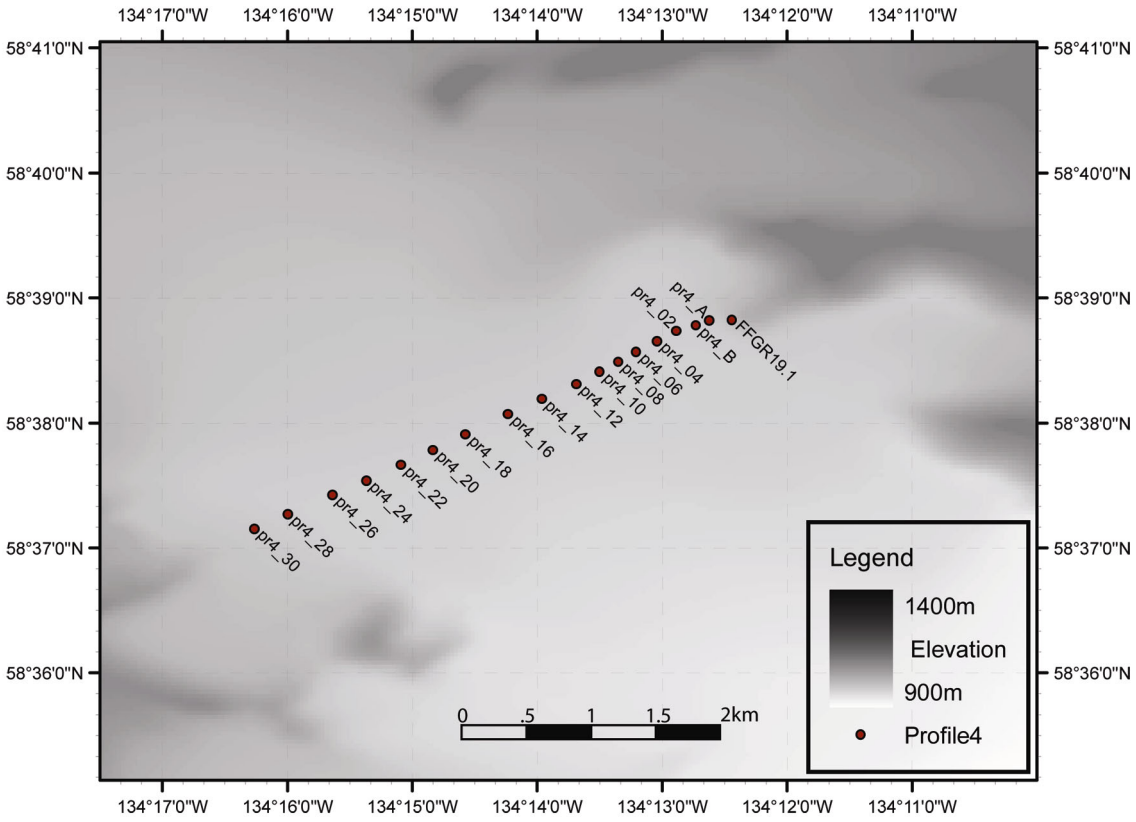

Figure 5. Locations of gravity observing stations in Profile IV. Location of Profile IV shown in Figure 1. Background image is a Digital Elevation Model.

Equipment

The gravimeter used was LaCoste and Romberg Model G, no. 129, belonging to the California State Department of Natural Resources. The gravimeter was not self-leveling, so each reading required positioning the gravimeter on a dished platform and adjusting the level of the gravimeter with leveling screws in its base. When taking measurements on snow, especially in warm, sunny conditions, melting and shifting beneath the gravimeter caused difficulties in keeping the gravimeter level. This is a persistent problem in conducting gravity surveys on snow, and we tested various methods to create a stable platform. A broad plywood sheet proved too difficult to anchor firmly in the snow, and tended to slide and shift unacceptably.

The most successful platform proved to be a pair of skis turned upside down and stamped firmly into the snow (Figure 6). Their narrowness allowed them to be easily lodged in the snow, with the bindings and tips providing solid anchorage, while their

length kept the gravimeter from experiencing small, local shifts in the snow pack. Perhaps most importantly, the skis were always at equilibrium temperature with the snow, and so did not cause melting. Other platforms that we tried were at equilibrium temperature with the air, and thus caused melting that resulted in instability once in contact with the snow.

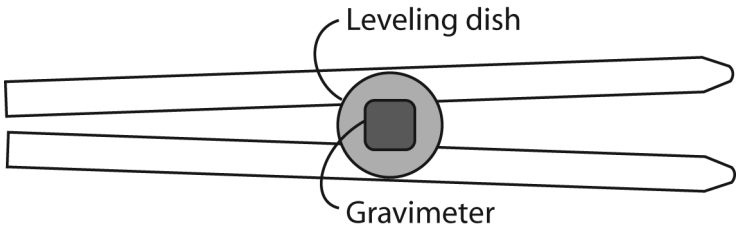

Figure 6. The most stable arrangement for conducting gravity measurements on snow. The gravimeter's leveling dish was placed on the bases of two skis inverted and packed into the snow.

Field Work

We took our measurements over two days using the practice of looping, whereby a series of stations is visited in sequence and the loop is closed by reoccupying the first station of the sequence (Isherwood, 2004). Closing the loop allowed for calculations that eliminate the effect of drift. Over sufficiently short time intervals, earth tides can be taken as a linear variation, so their effect will also be eliminated by the drift calculations. On the first day of observations, we visited the first nine stations of Profile IV in a loop taking four hours. On the second day, we visited the last six stations, with the last station of the previous day serving as the starting and ending station of this second loop. This loop took three hours to complete. A third loop consisting of the two additional eastern stations took one hour to complete.

The gravimeter provided only relative gravity measurements, so survey marker FFGR19.1, located on bedrock adjacent to Profile IV, served as a reference station (Figure 5). We computed all readings on the glacier relative to readings at FFGR19.1.

The drift calculations used here relied on the assumptions that the drift is linear and that the readings taken at the station that starts and ends each loop form endpoints of this linear drift. The following equation gives the time-weighted change in gravity

between the readings at the starting/ending station and the readings at an observing station, thus accounting for drift (Isherwood, 2004).

$$\frac{\sum_{i=1}^{n} \frac{\Delta g_i}{\Delta T_i}}{\sum_{i=1}^{n} \frac{1}{\Delta T_i}} \tag{1}$$

where n is the number of ties between an observing station and the starting/ending station. That is, when $i = 1$, Δg is the difference in the gravimeter readings, and ΔT is the separation in time, between the *first* reading at the starting/ending station and the reading at the observing station. When $i = 2$, Δg and ΔT are the differences between the *second* reading at the starting/ending station and the reading at the observing station. If more than two ties exist between two stations, n represents the number of ties.

Two observers, Mordecai and the author, took measurements at each station, but we computed the drift calculations separately for each observer's readings in order to remove the effects of any systematic operator bias (Isherwood, 2004). With two observers using the practice of closing loops, the final gravity value at each station represented the combination of four ties between the station and the starting point of the loop.

These computations referenced the readings at each observing station to the starting/ending station of each loop. Further referencing the readings at the starting/ending stations to the reference station FFGR19.1, using the same method, put the data in the following form: the gravity readings at each station represented the difference in gravity between station FFGR19.1 and the observing station.

We took the observational error in the gravimeter readings to be ±0.1 mgal. The machine accuracy was reported as ±0.01 mgal, so the total uncertainty in gravimeter readings was ±0.11 mgal.

Data Reduction

In order to obtain the Bouger anomaly from the data, I subtracted the observed gravity at each station from the theoretical gravity calculated for that station. The theoretical gravity is given by

$$g_{theo} = g_0 + g_f + g_B + g_T \quad (2)$$

where g_0 is the theoretical value of gravity at mean sea level, g_f is the free-air correction, g_B is the Bouger slab correction, and g_T is the terrain correction (LaFehr, 1991). Latitude determines value of g_0, which is found using the International Gravity Formula. Elevation determines the free-air correction, and elevation and bedrock density determine the Bouger slab correction. Elevation and latitude data for the stations in Profile IV were very accurate owing to the high quality GPS equipment used, so g_0 and g_f had negligible uncertainty. The uncertainty in the Bouger slab correction g_B was determined by the uncertainty in the density of the bedrock under the glacier. The coast range batholith that underlies the Icefield is composed of granodiorite (Miller, 2004). Granodiorite has a range of possible densities of 2.67-2.79 g/cm^3 (Dobrin and Savit, 1988). This corresponds to a 6 mgal change in g_B, so the uncertainty in g_B was ±3 mgal.

I computed terrain corrections by hand using the method of Hammer (1939). A more recent discussion of terrain corrections is given by Nowell (1999). I considered the terrain effects for zones B through K, corresponding to distances from 2 m to 9.9 km, on USGS Topographic maps in 1:63,300 and 1:250,000 scales. The most important station at which to compute a terrain correction was the reference station, FFGR19.1. This station was located on bedrock featuring significant topographic variation (see Photograph 2), and thus had a larger terrain correction than the stations located on the glacier. Additionally, its readings served as reference values for all other stations. The best estimate of a terrain correction at FFGR19.1 was 4.145 ± 0.8 mgal.

For stations on the flat surface of the glacier, the terrain corrections and uncertainties were much smaller. The inner zones, B through D (2-170 m), had zero contribution because the terrain immediately surrounding the stations was completely flat. For stations on the eastern half of Profile IV, there was some contribution in zones E though H (170-1500 m) from the bedrock at the eastern edge of the glacier, but this

tapered to zero for stations closer to the center of the glacier. The outer zone corrections were approximately the same for all stations, around 1 mgal. For all stations on the glacier, the terrain correction was between 0.93 mgal and 1.4 mgal, with uncertainties between ±0.2 mgal and ±0.3 mgal.

A regional gravity gradient must often be accounted for in gravity surveys, but it was not possible to find out if such a gradient existed at Profile IV. The standard procedure to determine the regional gradient along a profile is to take observations on bedrock on opposite sides of the valley, where the anomalies are small and nearly equal, and take the change in gravity (after applying reductions) to be the regional gradient along the profile. This gradient can then be subtracted from the anomaly. This was not possible on the Taku because the western side of the glacier was inaccessible due to crevassing. This led to the possibility of an undetermined error in the data that was largest at the westernmost stations and zero at the easternmost stations. However, the high degree of smoothness and symmetry in the data suggested that any such error was small. Additionally, regional gradients are often caused by changes in bedrock type, while the bedrock under the Icefield is largely of a single type.

An additional complication was due to the proximity of the reference station FFGR19.1 to the glacier. It was less than 100 m from the edge of the ice, so there was an anomaly present in the measurements taken there. In order to extract a true Bouger anomaly from relative gravity data, the measured gravity at the reference station must be equal to the theoretical gravity, but this is not the case when there is an anomaly present in the measurements at the reference station. Thus, the anomalies derived were actually anomalies *relative* to FFGR19.1. These under-predicted the actual Bouger anomalies by the amount of the anomaly at the reference station (Figure 7). Equation (2) could not be applied to find the value of this anomaly, because the gravity readings at FFGR19.1 were the reference values for all other stations.

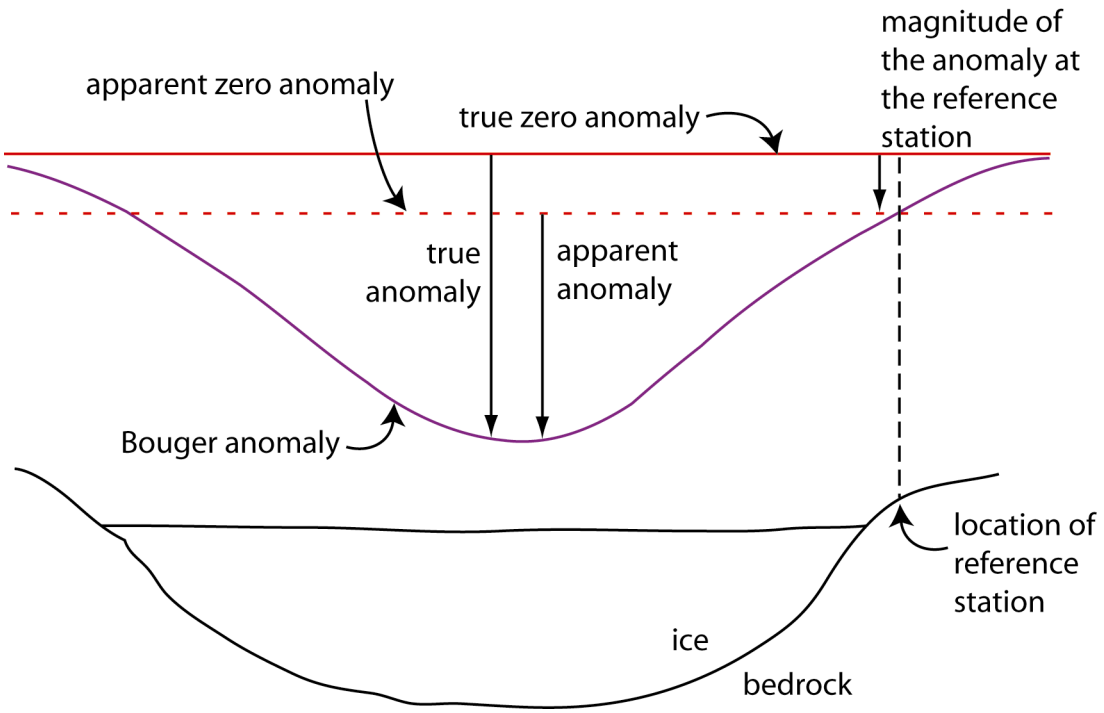

Figure 7. Cartoon showing that a gravity anomaly extends beyond the boundaries of an anomaly-causing body. If the reference station for a relative gravity survey is located off the glacier but within the zone of the anomaly, the effect will be to reduce the apparent anomaly at each observing station by the magnitude of the anomaly at the reference station.

This phenomenon could be corrected for during forward modeling: the Bouger anomaly at FFGR19.1 could be calculated by the forward model and subtracted from the model-derived anomaly at each station. This turned each anomaly calculated by the forward model into an anomaly relative to the base station anomaly. This was the form of the observed data, so the model and Bouger anomalies could be compared. The anomaly calculated by the forward model at the base station was around 15 mgal, so ignoring this effect would have led to a significant under-prediction of ice thickness. Since the Bouger anomaly was relative to the base station anomaly, and was thus ~15 mgal less than the true Bouger anomaly, it will be described from here on as the *relative* Bouger anomaly (Figure 8).

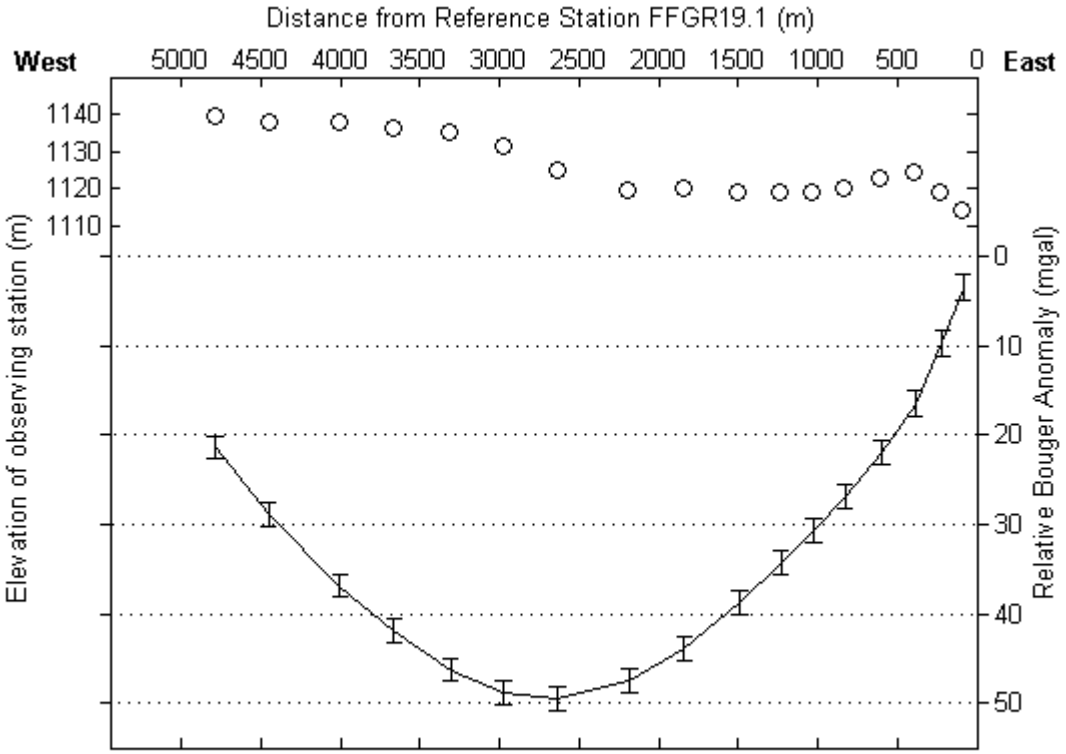

Figure 8. Locations and elevations of gravity observing stations in Profile IV, with corresponding terrain-corrected Bouger anomalies. Anomalies are relative to FFGR19.1.

Modeling

In order to determine the shape and thickness of the Taku Glacier such that it could cause the observed relative Bouger anomaly, I created a forward model of the gravitational effects of a glacier.

Many approaches exist for modeling the gravitational effects of subsurface bodies. Those used here were two-dimensional, which means they rely on the assumption that the body in question is infinite in the third dimension. That is, the two-dimensional body is taken to be the cross section of a prismatic body. This was a very reasonable approximation for a glacier, especially a large glacier like the Taku, which extends straight for ten kilometers or more on either side of Profile IV. However, the edges of the glacier are not straight, and irregularities there hurt the assumption of an

infinite third dimension. This caused some uncertainty in the model, and created a problem in assigning a width to the model glacier.

The location of the eastern edge of the glacier was well constrained because we approached from the east and had survey data there, but the inaccessibility of the western edge of the glacier meant that we could only estimate its location. As a result, the location of the western edge, and by implication the width of the glacier, were not well known. Even an exact measurement of the distance from eastern bedrock to western bedrock would not necessarily have been the most appropriate width to use in the model, since it was unlikely that the surface width at an arbitrary location would represent the width for which the assumption of an infinite third dimension was most valid.

In order to find the most appropriate width to use in the gravity model, I fit curves to the anomaly data to extrapolate a location on the western side of the glacier that would have the same anomaly as that found at the easternmost station, which was within 100 m of the glacier's edge. This relied on the assumption that the anomaly was symmetrical; if true, then the ice thickness at the easternmost station and at the extrapolated western station would be equal, and the distances to the respective edges would be equal. The assumption of a symmetrical anomaly and by implication a symmetrical valley was reasonable for a glacially carved valley.

Simple curves fit the data very well. A quadratic, least squares fit had an R^2 value of 0.9976, while a single sine curve had an R^2 value of 0.9930. The two curves predicted distances of 5290 m and 5313 m from FFGR19.1, respectively, for the extrapolated location of a western station having the same anomaly as the easternmost station (Figure 9). Adding the distance from the easternmost station to the eastern edge implied a value of 5.4 km as the width of the Taku most appropriate for the gravity model.

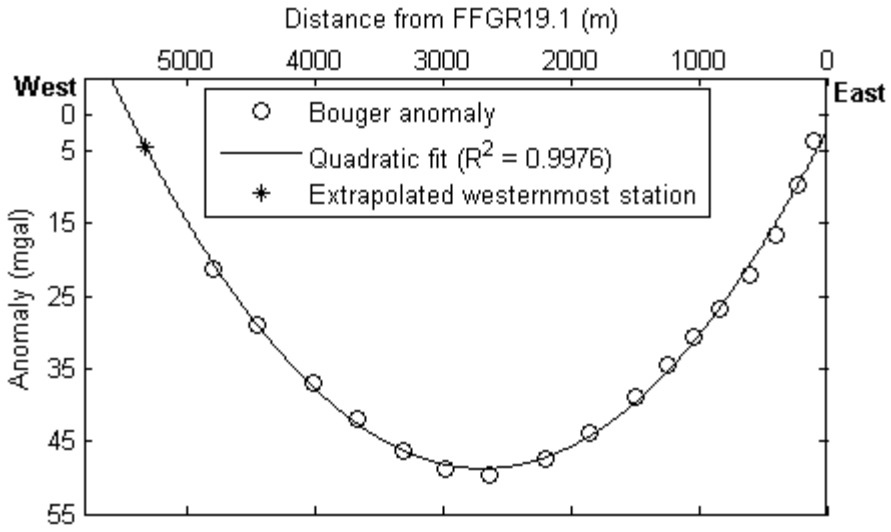

Figure 9. A quadratic curve fit to the relative Bouger anomaly indicated a location on the western side of the glacier that would experience the same anomaly as the easternmost station. This determined the width of the glacier used in the model.

A convenient model for a glacial cross section is a series of rectangular columns (Figure 10). The gravitational effect of the entire body is the sum of the effects of each block. The formula for the gravitational anomaly caused by a rectangular block that is infinite in the third dimension is given by Heiland (1940) (pp. 150-152).

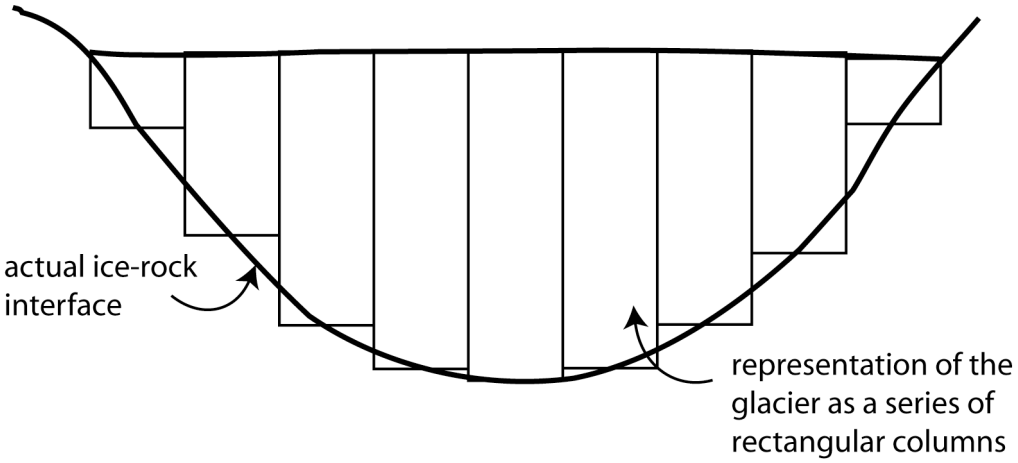

Figure 10. Cartoon showing a glacial cross section modeled as a series of rectangular columns.

$$\Delta g = 2G\delta[x_2 \ln\sqrt{\frac{D^2+x_2^2}{d^2+x_2^2}} - x_1 \ln\sqrt{\frac{D^2+x_1^2}{d^2+x_1^2}} + D(\tan^{-1}\frac{x_2}{D} - \tan^{-1}\frac{x_1}{D}) - d(\tan^{-1}\frac{x_2}{d} - \tan^{-1}\frac{x_1}{d})]$$

(3)

where $G = 6.67\times10^{-11} m^3 kg^{-1} s^{-2}$

δ = density contrast in kg/m^3

x_1 = horizontal distance from station to near edge of block

x_2 = horizontal distance from station to far edge of block

D = depth from station elevation to bottom of block

d = depth from station elevation to top of block (d<0 if top of block is above station elevation)

(Note: Result is in m/s^2. Multiply by 10^5 for milligals.)

(see Figure 11)

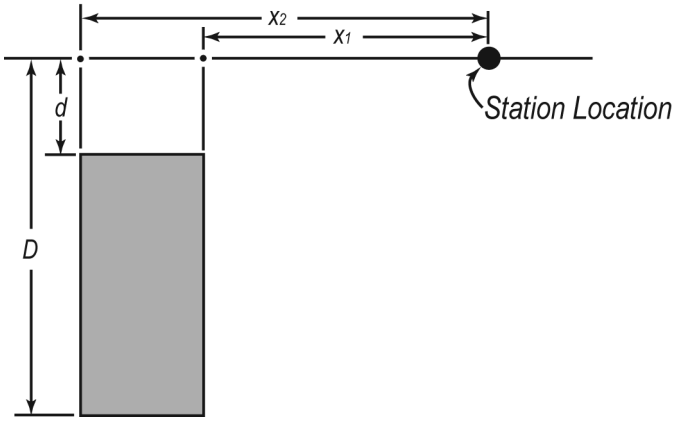

Figure 11. Variables used in Equation (3).

The density contrast used here for modeling was 1.82. This was determined by the average density of granodiorite, 2.72 g/cm^3 (Dobrin and Savit, 1988), and the average density of temperate glacier ice, 0.90 g/cm^3 (Miller, 2004). Different density contrasts in practice showed only a small influence on the results of the forward model.

The first step of the modeling process was to divide the width of the glacier into a series of equal width columns. The narrower the width, the more columns, and thus the greater the resolution of the final model; however, a very large number of columns made

the model poorly constrained by the data, so I chose the number of columns arbitrarily to match the number of observing stations. On the Taku, there were 17 stations. Seventeen columns over a span of 5.4 km yielded a column width of ~320 m.

The forward model could be used to calculate the gravity anomaly at any *x*-*z* location in the plane of the cross section, but for comparison with the observed data, the forward model calculated anomalies at the locations of the observing stations.

Finding the terms *D* and *d* required knowing the elevations of the station locations and of the column tops. The column tops were constrained to lie at the surface of the glacier. The survey data gave elevations for the observing stations, and linear interpolation of these elevations gave the elevations of the column tops. Depths were defined to be positive below the plane of the station and negative above the plane. Finding *D* required assigning thicknesses to each of the columns, but this column thickness corresponded to the thickness of the glacier, which was the desired result of the modeling process. A simple approach to this problem would be to guess initial column thicknesses, run the forward model, and iteratively solve for them by manually manipulating them to give a better fit with the observed data. One problem with this approach was that it would be time-consuming and inefficient; another was that gravity anomalies are non-unique, so no single depth profile can be the unique solution to a gravity anomaly.

Solution to the problem of non-uniqueness

By manually manipulating the array of depth values that serve as the input to the forward model, it is possible to arrive at a reasonably good fit with the relative Bouger anomaly. An automated approach can quickly test several thousand variations to a starting array and keep the best fitting array, determined by the misfit, $\Sigma\left|g_{obs} - g_{theo}\right|$, between the observed anomaly and the model-derived anomaly. However, this single best-fitting array is non-unique. An infinite number of possible combinations of column depths can generate the same anomaly profile. For this reason, a statistical approach was preferable.

Gravity anomalies are non-unique because gravity is determined by the density, shape, and depth of subsurface bodies. When all three of these parameters are allowed to

vary, an infinite number of combinations can create the same anomaly at the surface. In practice, one or more of these parameters can be (1) determined by other geophysical means or (2) inferred from regional geologic conditions (Heiland, 1940). In this case, I applied (2) by constraining the densities, making the observed Bouger anomaly a function of only shape and depth. There still were infinitely many combinations of these two parameters that could agree with the data, but additional constraints narrowed them down. I assumed, from the regularity of the Bouger anomaly, that there was only one anomaly-causing body, and I applied partial constraints to the shape and depth. The shape of the cross section had to be geologically reasonable; highly irregular cross sections could be discarded. The depth unknown is generally for a completely buried body; in this case, the top of the glacier was constrained to lie at the surface, so the depth unknown was only to the bottom edge. Thus, although infinitely many variations of the shape and depth of the ice-bedrock interface could generate agreement with the data, these variations would lie within a certain range.

To solve the problem, I found several thousand viable depth arrays and analyzed them as a group. To do this, I used a Monte Carlo approach whereby a program generated a large number of random variations of an initial array of depth values, then used the forward model to find the anomalies caused by each array. The arrays whose anomaly fell within the uncertainty bounds of the observed data were kept.

Two arrays served as starting points in two different trials, Trial A and Trial B (Figure 12). The starting array in Trial A was based on gravity data alone, with no constraints from other sources. The intention was to test the gravity modeling process as if it was conducted in the absence of other geophysical information. The extent to which the results of this trial converged with the results of the seismic migration would indicate the reliability of gravity surveys as a stand-alone method of geophysical investigation for use in previously unstudied areas. It also served as a control case with respect to the structure of the cross section, since it could test whether a smooth starting array could generate any of the irregular structures seen in the seismic results, such as a plunging center and berm levels. With this in mind, the cross section was as close as possible to a typical U-shaped glacial valley, and was as smooth and symmetric as possible to avoid biasing the results with the presence of irregular structures. I ran it through many tests

with the forward model and manually manipulated it to have a good initial fit with the relative Bouger anomaly. The starting array in Trial B had depths corresponding to the ice thicknesses from the re-migration of seismic data. The intention was to see how well the cross section from the seismic migration agreed with the gravity data, and to test the convergence of the two gravity modeling trials.

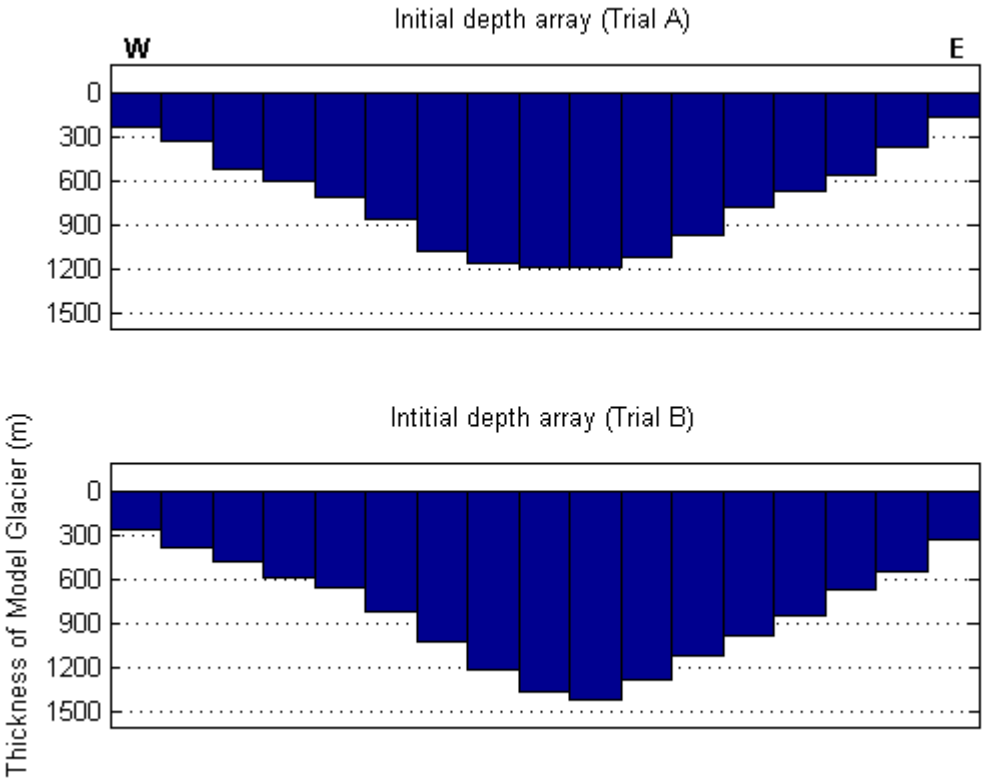

Figure 12. The two initial arrays for Trials A and B. The upper cross section was based on gravity data alone. It was intended to represent a typical U-shaped glacial valley and was as smooth and symmetric as possible to avoid biasing the results. The lower cross section was based on the seismically-derived cross section of Profile IV.

These starting arrays were randomized by varying each element in the array within a normal distribution having a standard deviation of 0.224. This variance was large enough to yield a high a percentage of geologically unreasonable arrays (discussed below) that agreed with the data, but I chose it to avoid biasing the results too much towards the initial depth array. If the variance was too small, the random variations would all resemble the initial array too closely, and the result might not be useful. Too

large a variance would create such erratic arrays that finding solutions would be very slow. A standard deviation of 0.224 was a compromise between these two factors.

The Monte Carlo routine operated by using the forward model to find the anomaly caused by each random array. For each array, if the anomaly at each station fell within the bounds of the observational uncertainty in the observed data, then it was kept. However, not all of the arrays that met the selection criteria were geologically reasonable. Because of downward continuation, some very implausible arrays generated smooth anomalies. In order to remove the geologically unreasonable arrays, all of the arrays were sorted by their roughness and some percentage was kept. The roughness of each array was given by

$$\sum_{i=1}^{n-1} \left| Z_i - Z_{i+1} \right| \tag{4}$$

where Z is the depth, i is the observing station, and n is the number of stations. These results are presented below (see RESULTS).

Seismic migration

For comparison with the results of the gravity modeling, I re-migrated the seismic data collected in a 1994 reflection survey (Sprenke *et al.*, 1994). As discussed in the INTRODUCTION, the original migration of this data was done mostly by hand. The timing and slopes of reflectors were picked out on hardcopies and calculated by hand, and this timing data was migrated in a spreadsheet. For the re-migration I sought to obtain more accurate timing data. The digital records could not be located, so I scanned the original paper records into digital images and digitized the clear reflections. The images were skewed due to warping and wrinkling of the paper records and imperfect alignment during scanning. To correct for this I cropped and skewed each reflection in order to ensure that the timing lines were horizontal in the immediate neighborhood of each reflection. I then digitized all strong reflections with digitizing software by manually picking the arrival times of clear reflections at each geophone. This produced digital timing data.

A flaw with this process was the possibility of neglecting reflections, since I picked reflections by visually inspecting the records and identifying strong reflectors by

eye. However, reflections were generally very strong (Figure 13), and I was able to find enough to generate a useful cross section. Approximately 20 percent of the records had no identifiable reflections, so I digitized none of these. In the original analysis, reflections were sometimes extrapolated from records with strong reflections into adjacent records that lacked clear reflections of their own. Because I did not do this, my cross section had fewer data points than the one generated in 1994.

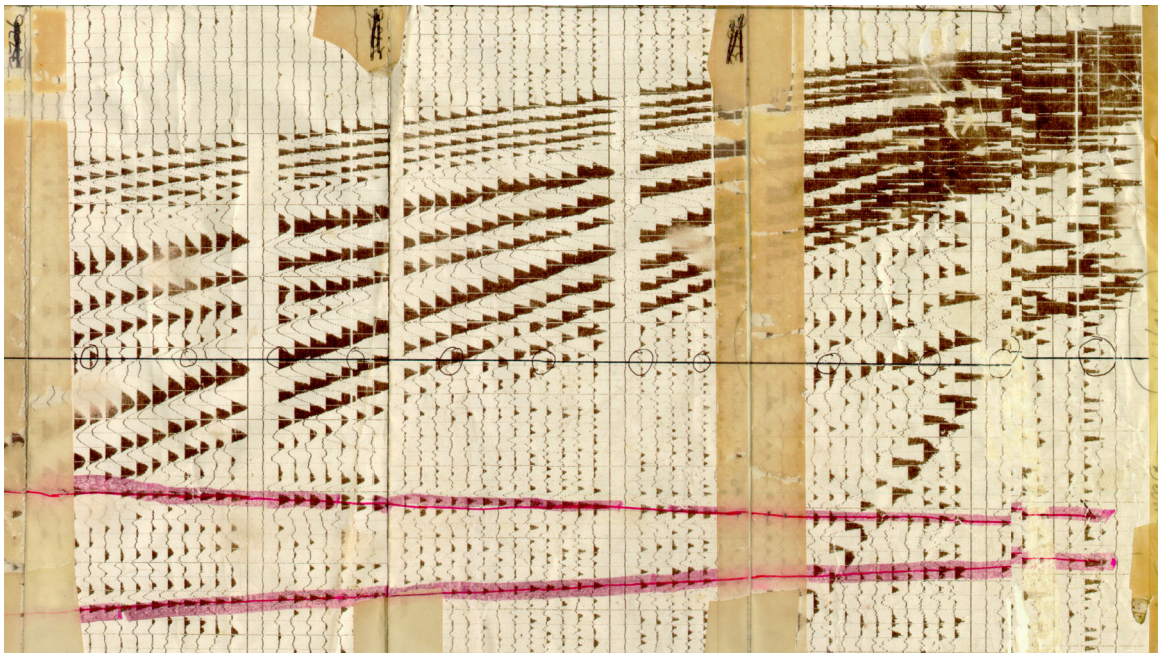

Figure 13. Three seismic records showing two clear reflections (highlighted in pink) that are continuous across all three records. The shot point is located in the upper right.

Using the digital timing data, the following hyperbolic relationship could be applied (Dobrin and Savit, 1988):

$$V^2T^2 = X^2 + (4H\sin\phi)X + 4H^2 \qquad (5)$$

where V is the compressional wave velocity in ice, taken to be 3660 m/s (Miller *et al.*, 1993)

T is the travel time (known)

X is the distance from shot to receiver (known)

H is shortest distance from the shot point to the reflecting plane (unknown)

ϕ is the dip of the reflecting plane (unknown)

Fitting this hyperbola to the X and T data for each reflection yielded values for H and ϕ. This allows one to find the location in the vertical plane of each reflector, using the following geometric relationships (Figure 14) (Sprenke, 2004):

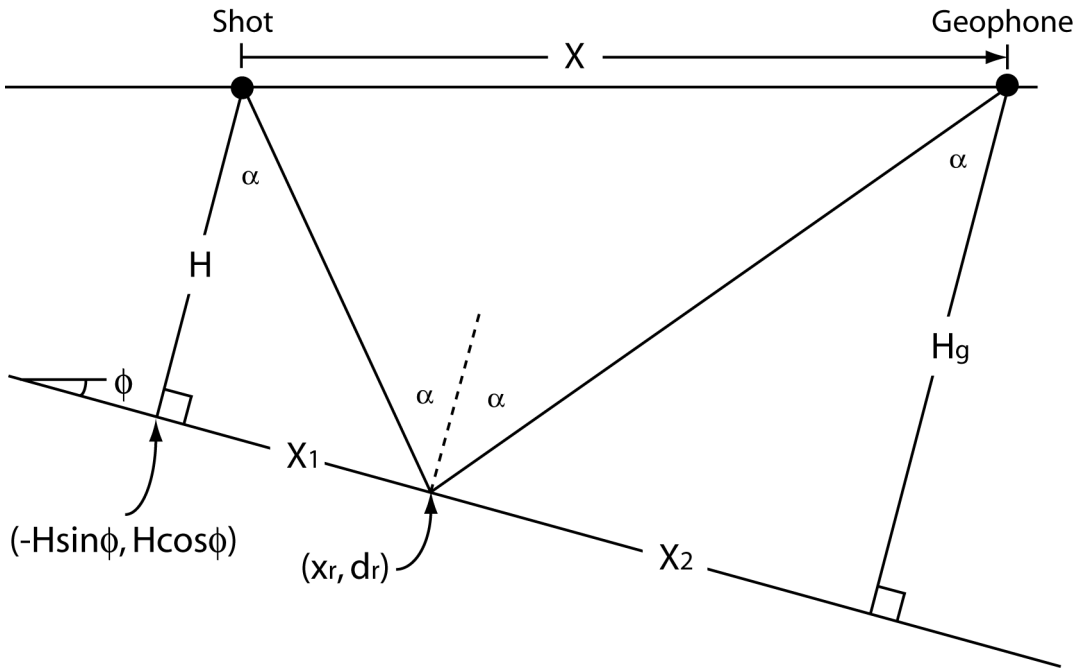

Figure 14. Assumed reflection geometry, where (xr, dr) is the coordinate of the reflecting point.

$$\frac{H}{H_g} = \frac{X_1}{X_2} \text{ (by similar triangles) or } X_2 = \frac{H_g}{H} X_1 \qquad (6)$$

$$X_1 + X_2 = X\cos\phi \text{ or } X_2 = X\cos\phi - X_1 \qquad (7)$$

Combining (6) and (7) gives $\frac{H_g}{H} X_1 = X\cos\phi - X_1$ or $\frac{H_g}{H} X_1 + X_1 = X\cos\phi$.

Solving for X_1 gives $X_1 = \frac{XH\cos\phi}{H_g + H}$. (8)

With H_g given by $H_g = H + X\sin\phi$, all the variables in (8) required to find X_1 are known. The coordinates of the reflecting point, (x_r, d_r), can then be expressed in terms of the known values X_1, H, and ϕ:

$$x_r = -H\sin\phi + X_1\cos\phi \qquad (9)$$

$$d_r = H\cos\phi + X_1\sin\phi \qquad (10)$$

The final migrated cross section is shown in Figure 15. Some reflectors, indicated in gray, did not fit well with the majority and may be the result of incorrectly picked weak reflections. Others, particularly the cluster located on the western side of the valley, may be the result of out of plane reflections.

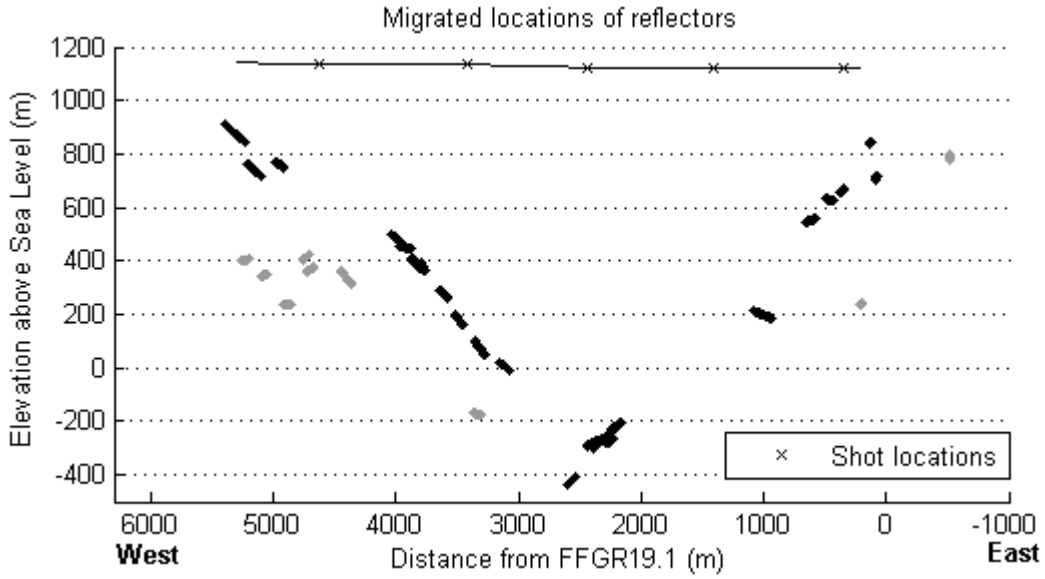

Figure 15. Cross section of Profile IV based on re-migration of 1994 seismic data. There was a large concentration of reflectors at 200-300 m below sea level. Light gray denotes weaker reflections, possibly due to out of plane reflection.

The compressional (P-wave) velocity in ice used in the migration equations was 3660 m/s^2. There is some uncertainty in the literature for this value. In polar ice, it is known to vary with temperature, but in temperate ice, it varies with water content (Miller *et al*., 1993). For this reason the value is specific to a location, and should be determined for each study site. Using radio echo sounding in conjunction with seismic reflection, Miller *et al*. (1993) determined that 3660 m/s^2 was the most appropriate value for the Juneau Icefield. The authors also indicated that this experimental value was consistent with values cited in the literature for sites in Southern Alaska and British Columbia.

RESULTS

The Monte Carlo routine for fitting the gravity data ran with very different efficiencies in each of the two trials. In Trial A, when the starting array was manually manipulated to have a good initial fit with the relative Bouger anomaly, the program tested 1.6 million variations and found 3,110 that matched the data. In Trial B, when the starting array consisted of the seismic depths, the initial agreement with the observed data was not as good, and after 10.3 million variations, only 124 were found that matched the data. However, the anomaly calculated for these starting depths did not have a poor fit with the relative Bouger anomaly (Figure 16). The largest discrepancy between the calculated anomaly and the uncertainty bounds on the observed data was 1.5 mgal on the eastern half of the profile and 4.2 mgal on the western half. This suggests that the seismic and gravity data were in agreement with one another (see DISCUSSION), but it also revealed the weakness of the Monte Carlo method for efficiently handling a starting array that did not have an excellent fit with the data (see *Recommendations*).

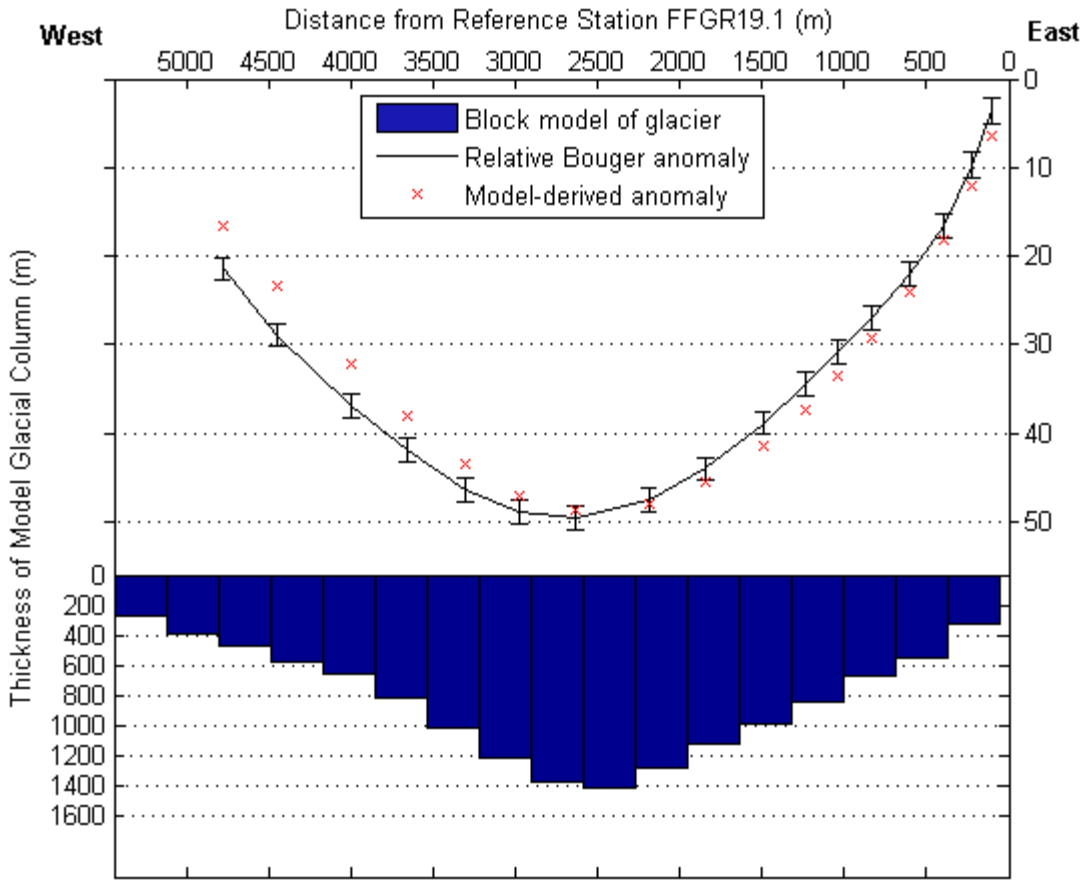

Figure 16. Cross section of Profile IV based on seismic results, and the corresponding relative anomaly calculated by the forward model.

Of the 3,110 arrays found in Trial A and the 124 found in Trial B, most were highly irregular and therefore geologically unreasonable, so I sorted the depth arrays by roughness, as described above. Breaking the arrays from Trial A into deciles based on roughness revealed that only the top two deciles contained geologically plausible arrays (Figure 17). The roughest 80 percent were discarded. In Trial B I kept the smoothest 30 of the 124 arrays (Figure 18).

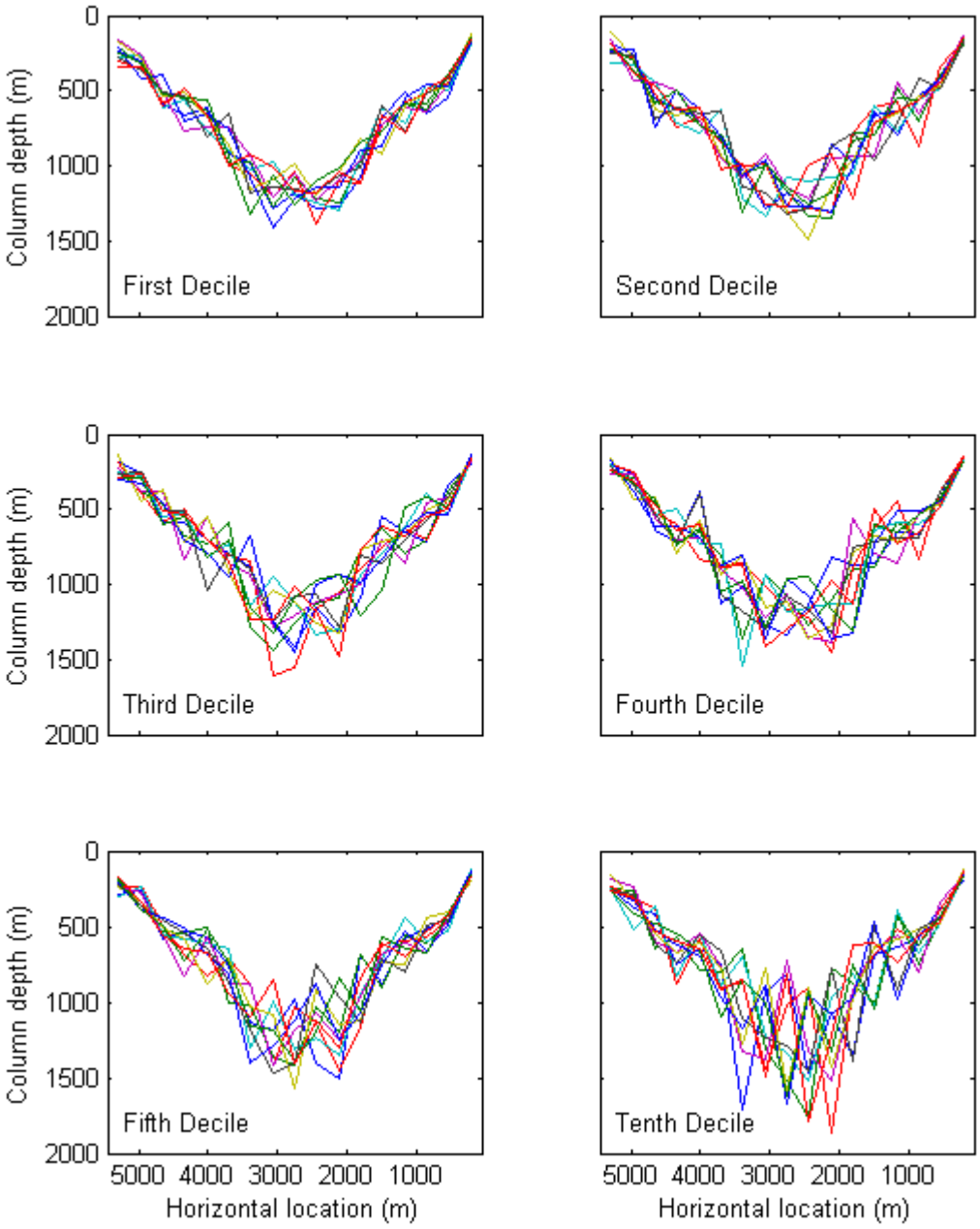

Figure 17. Ten randomly selected depth arrays from several roughness deciles of the entire set of arrays generated in Trial A. Ranking all arrays by roughness and breaking them into deciles revealed that most were too irregular to be geologically plausible. I chose to consider only arrays from the top two deciles; all others were discarded. Colors in this figure are only to distinguish between arrays.

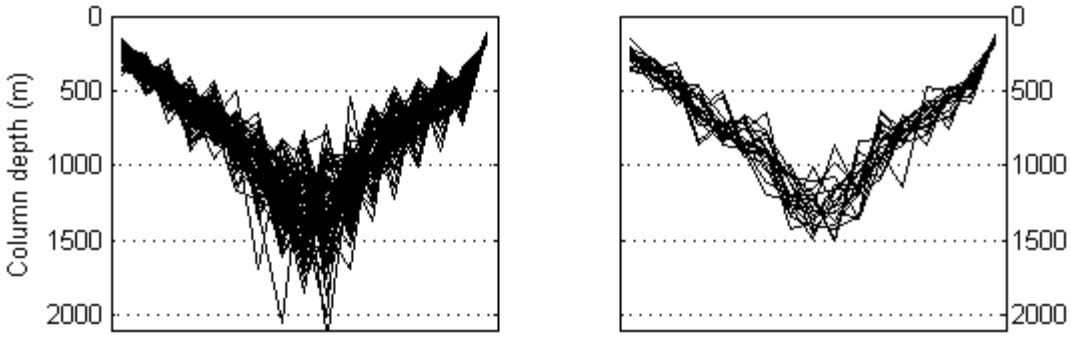

Figure 18.
Left: All 124 depth arrays generated in Trial B.
Right: The 30 smoothest of these arrays.

After this selection was completed, there were 622 arrays left from Trial A and 30 left from Trial B. I took the median of each of these sets to be the final representation of Profile IV for that trial. The median was preferable to the mean because it is less sensitive to outliers. Outliers occurred less frequently when the roughest arrays were removed, but were still present. The Median Absolute Deviation (MAD) defined the uncertainty for each column. The MAD is given by

$$median\left|Z - Z_{median}\right| \tag{11}$$

and was applied separately to each column of the glacier model.

Cross sections generated

In Trial A, the final cross section had a thickness of 1214±89 m at its deepest point (Figure 19). The upper bound on this depth, 1303 m, was approximately 100 m shallower than the depths suggested by seismic work. The uncertainty of 89 m was the Median Absolute Deviation. The cross section was U-shaped, similar to the starting array.

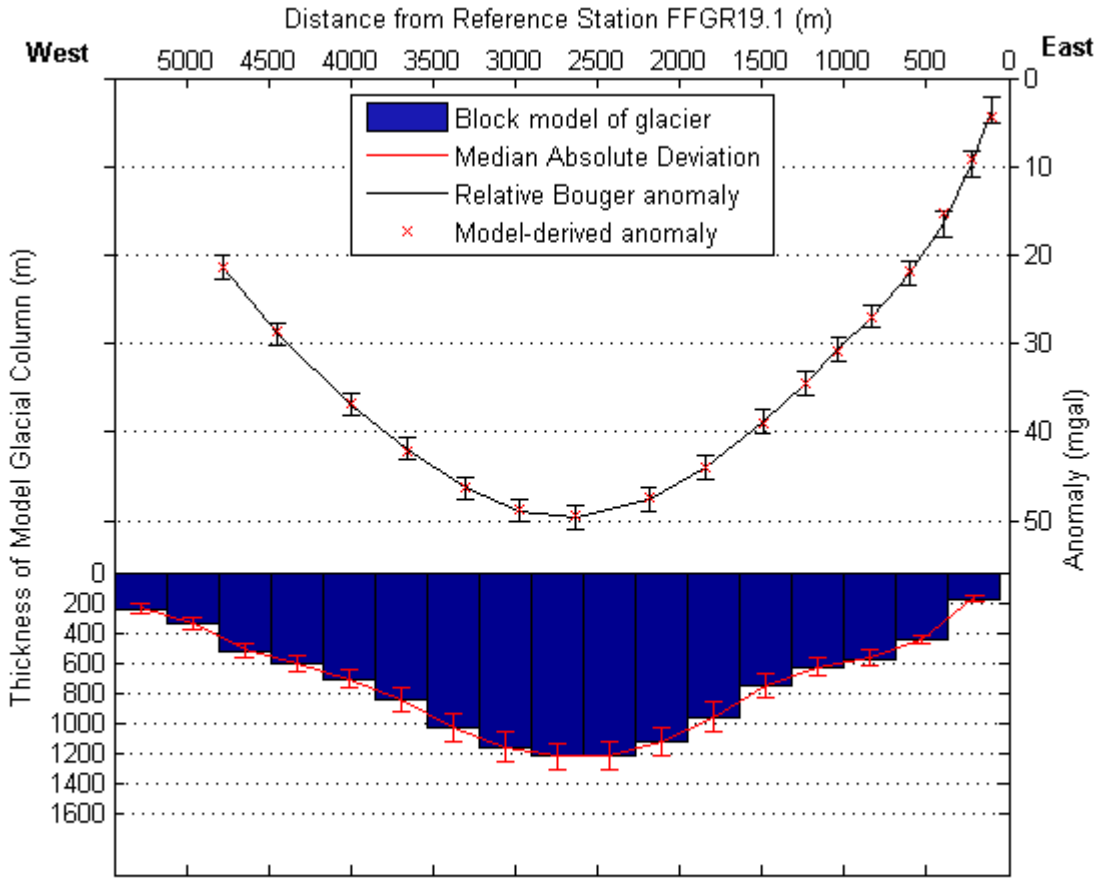

Figure 19. Cross section of Profile IV determined by gravity modeling (Trial A). The thickness of each column is the median of 622 values. Each side of the error bar for each column is the Median Absolute Deviation of these 622 values.

In Trial B, the final cross section had a thickness of 1328±93 m at its deepest point (Figure 20). This was 114 m deeper than the deepest point in Trial A, but the uncertainties in the two trials overlapped. The upper bound, 1421 m, was in agreement

with the seismic results. The cross section featured a 300 m change in elevation in the bedrock interface at a distance of 3300 m from the eastern edge. It is possible that this was a result of using only 30 arrays to compute the results of this trial, and if more were used, this feature would have been smoothed out. However, this feature was similar to features seen in the cross section of Sprenke *et al*. (1994) (Figure 4). These were hypothesized to represent berm levels from a previous glaciation, so it is possible that this is a genuine feature of the interface.

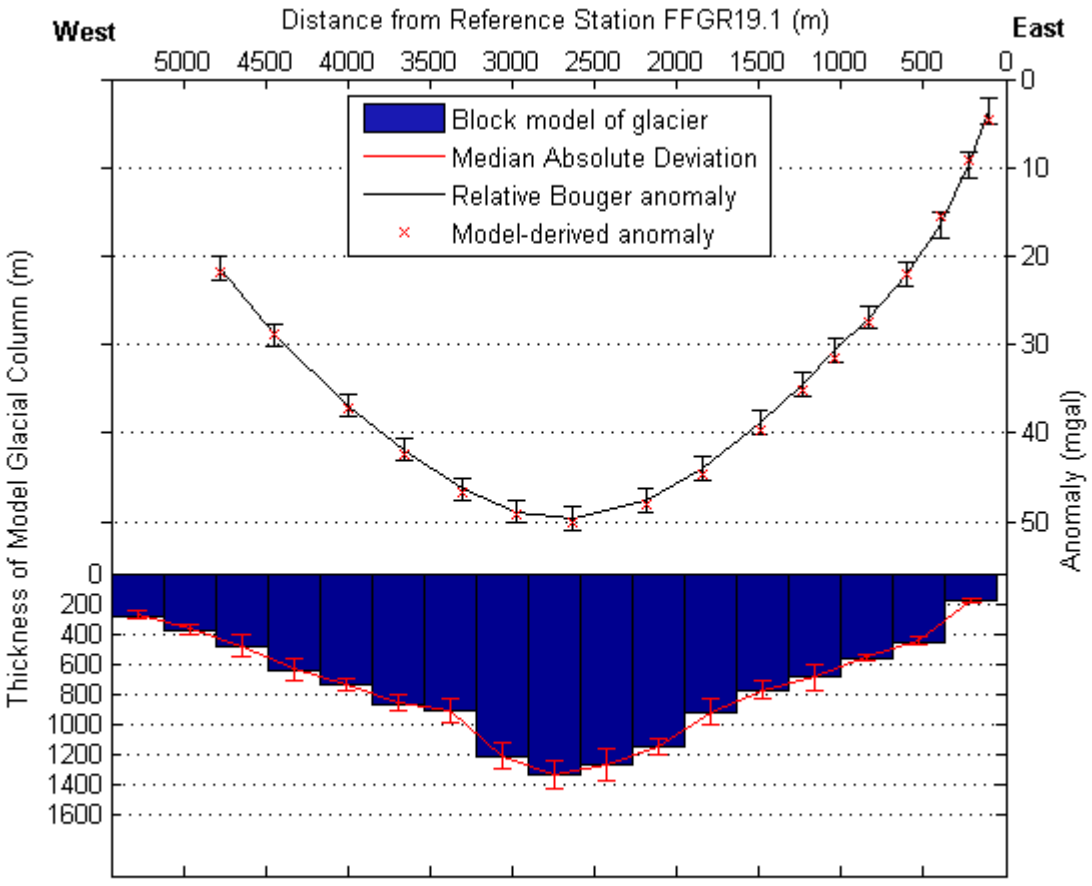

Figure 20. Cross section of Profile IV determined by gravity modeling (Trial B). The thickness of each column is the median of 30 values. Each side of the error bar for each column is the Median Absolute Deviation of these 30 values.

The initial depths used in Trials A and B are plotted with the final depths in Figure 21. The final cross section of Trial A closely matched its starting values, perhaps because the initial fit with the observed data was very good. The final cross section of Trial B differed from its starting values, which is not surprising since it did not have as good an initial fit with the data. However, it was unexpected that the greatest change between the initial and final cross sections occurred on the eastern side of the valley, since the western side had a worse initial fit with the relative Bouger anomaly (Figure 16). With the exception of the center region, the two final cross sections from Trials A and B had excellent convergence.

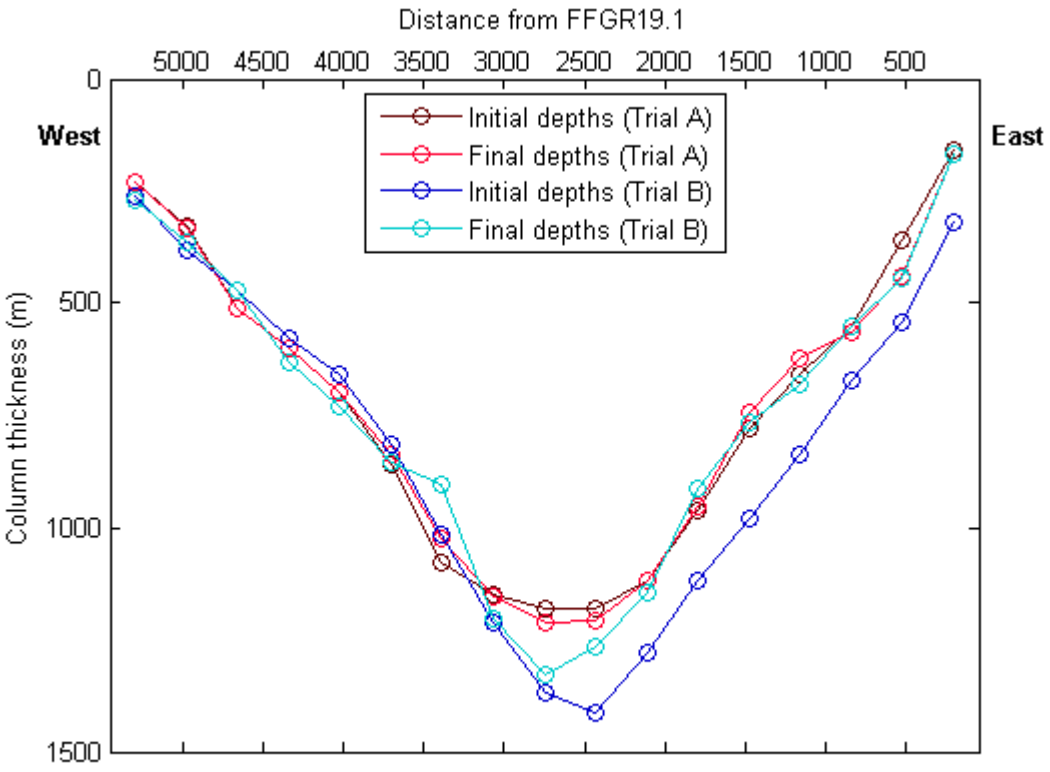

Figure 21. Initial and final depth arrays for Trials A and B showing how much the final solutions deviated from the starting values.

DISCUSSION

There are three issues of convergence to address: (1) the convergence of the results of the two gravity modeling trials, A and B, (2) the agreement of the seismically derived cross section with the relative Bouger anomaly, and (3) the agreement of the seismic interpretation of Profile IV with the gravity interpretation of Profile IV. All three represent important aims of this thesis, since (1) and (3) are tests of the gravity inversion method used and (2) is a test of the existing seismic work on the Taku.

(1) The convergence of the results of Trials A and B was excellent, with the exception of the deepest point of the glacier. This convergence suggested that the assumptions made to constrain the problem and the methods used to solve it had some success in overcoming the issue of non-uniqueness in gravity interpretation. Infinitely many variations of the bedrock interface could have generated the relative Bouger anomaly, but when the majority of these variations were eliminated on the grounds of geologic implausibility, the median of only several hundred variations successfully served as a good estimate of the shape and depth of the interface. The median of as few as several dozen variations even served reasonably well.

(2) The gravity anomaly calculated by the forward model for the seismically derived cross section agreed very well with the relative Bouger anomaly (Figure 16). This served as a confirmation of the recent seismically derived cross sections, since it showed that they are capable of generating the relative Bouger anomaly observed for the profile. Thus, a 1400 m deep glacier is consistent with the gravity data, even though that depth was not explicitly predicted by the gravity-based interpretation.

(3) The agreement was extremely good between the cross sections generated by the gravity modeling and the cross section determined by re-migration of the seismic data (Figure 22). The agreement was better on the western side of the profile than on the eastern side, although there were far fewer reflectors on the eastern side to use for comparison. The fit was worst in the center of the profile. In this region, a close-packed cluster of five seismic reflectors indicated a depth of 1400 m, while at the same location, the gravity modeling indicated depths of 1210±94 m (Trial A) and 1265±108 m (Trial B).

In addition, both gravity models suggested that the deepest point of the cross section was ~500 m west of this cluster of reflectors.

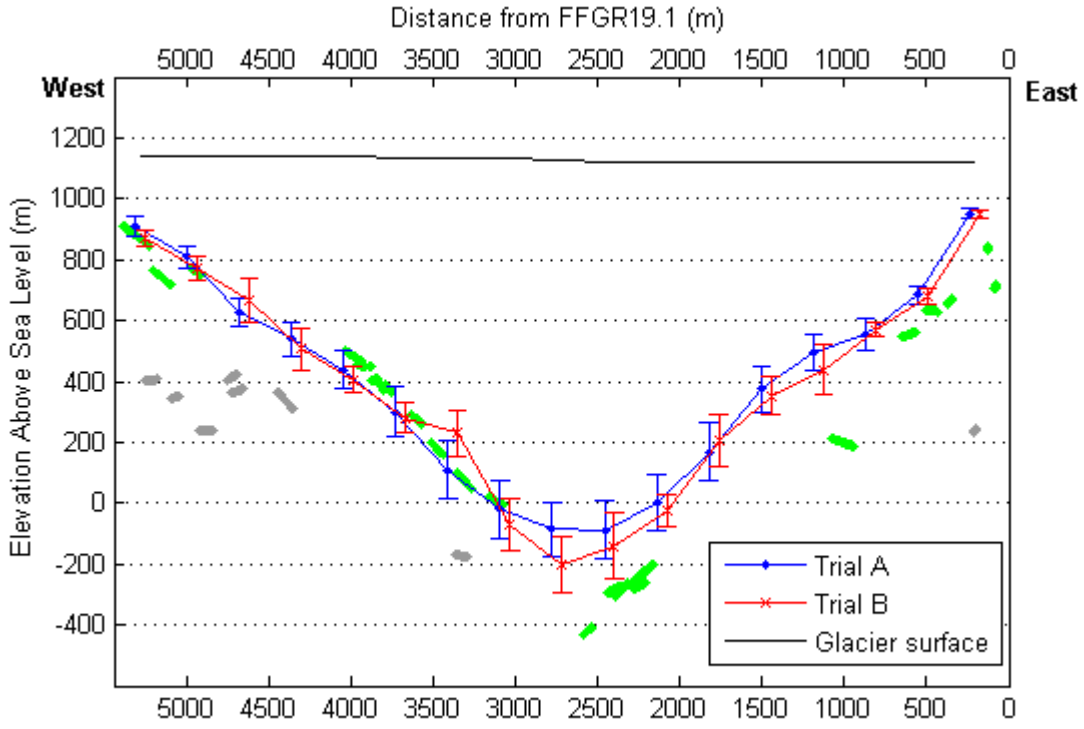

Figure 22. Cross sections of Profile IV from gravity modeling and seismic reflection. Green denotes strong, reliable reflectors; gray denotes weak or questionable reflectors.

The inability of the gravity data to resolve this deep center point is not necessarily problematic. If the reflection surveys were correct and the center of the glacier is indeed 1400 m thick, then the cross section will be V-shaped and its center will 'plunge,' as seen in the cross section of Sprenke *et al*. (1994) (Figure 4). It is not surprising that the gravity modeling failed to predict such a feature, since the gravity signals of sharp features are smoothed out at the surface. Even if the gravity data and modeling did not resolve the deep center, such a feature is not inconsistent with the data, as seen in Figure 16.

Since a gravity survey and a seismic survey would not be subject to the same errors, the agreement between the two methods served as a confirmation of the existing interpretation of Profile IV, as well as a validation of both the seismic and gravity

methods. This suggests that gravity surveys on the Icefield have the potential to generate cross sections as reliable and useful as those of seismic surveys. One drawback is that that gravity surveys may not be able to resolve sharp structures, but for flow modeling, the detailed structure of the interface is not as important as a good approximation of the cross-sectional area.

Recommendations

Several improvements could be made to the methods used here, although I do not know how substantial their effects would be. One is a refinement to the approximation of the glacial cross section as a series of rectangular columns. Applying a formula for the gravitational attraction of a triangular prism would allow the cross section to be represented as a series of trapezoidal columns, where each trapezoid consists of a rectangle with a triangular portion added to its base (Figure 23). This could potentially give the forward model greater precision.

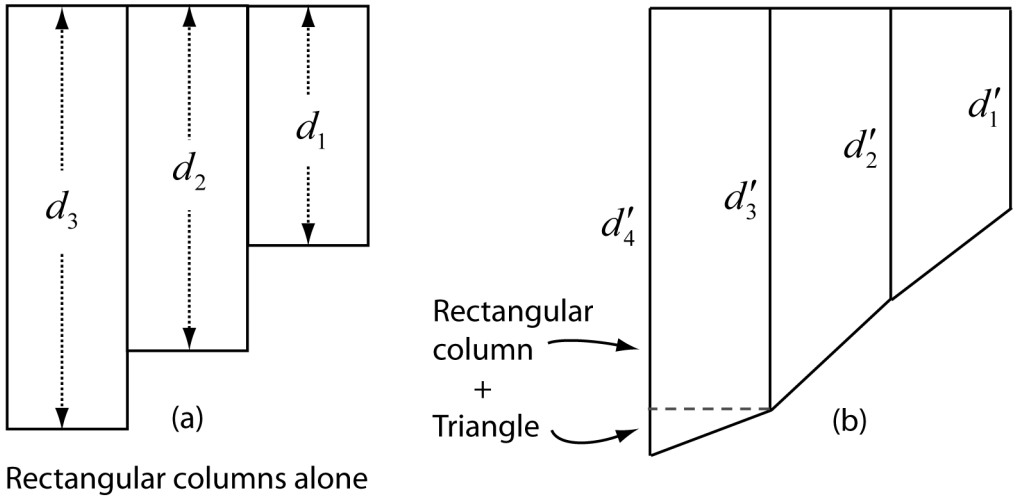

Figure 23. (a) The forward modeling scheme used here. (b) A more sophisticated approach. Adding a triangular portion to the base of each rectangular column would result in more precise forward model.

Another improvement would be to consider a low-velocity zone in the seismic migration. The seismic velocity in snow is substantially less than in glacial ice, so conducting seismic work on glaciers is analogous to conducting seismic work on bedrock

that is covered with a layer of sediments. Such a situation creates a low-velocity zone at the surface, which influences the travel times of seismic waves.

The change most likely to result in a substantial improvement in the quality of results would be a more efficient method for searching the parameter space when finding arrays that fit the data. The Monte Carlo method used here worked well when the starting array had a good fit with the data, but worked far more slowly when the fit was even slightly poor.

Additionally, adding more columns to the forward model and decreasing the column width accordingly would allow for greater resolution in the final cross section, but each additional column causes the parameter space to grow exponentially, so a more efficient searching routine would be required for this purpose as well.

Conclusions

The Juneau Icefield Research Program has studied the Icefield since 1949, and has a lengthy record of surface flow rates and mass balance data from measurements conducted during the summer field seasons. In the past decade, the use of high quality GPS equipment on the Icefield has resulted in very accurate measurements of surface flow rates and glacial surface heights. This equipment has also allowed for greater consistency in surveys from one year to the next, making year-to-year comparisons possible. This has the potential to provide a wealth of new and detailed information about the glaciers on the Icefield, but in order to obtain the greatest insights into their behavior, the quality of subsurface measurements must improve along with the quality of surface measurements. At present, fewer than 10 areas of the Icefield have undergone recent and reliable geophysical investigation. There is currently no program of subsurface investigation to parallel the well-organized and efficient program of surface surveying.

Each year more new areas of the Icefield are surveyed, but without information about ice thickness, the results of the survey team's measurements of surface velocity and height change are less informative, and the full potential of the data is not being realized. A program of geophysical investigation to accompany the surface surveying would result in richer and more informative data about the Icefield.

Gravity work could be an important component of such program. It is faster, easier and safer than seismic work. It requires no supplies or expenses other than the gravimeter itself. Although great care must be taken when transporting a gravimeter, it can be carried safely on a small over-snow vehicle, and a team of as few as two individuals can conduct a complete survey in two days or less. With this in mind, it would be feasible to envision a program of gravity investigation on the Icefield. The survey team annually visits many transverse and longitudinal profiles on the Icefield, and each profile surveyed by GPS provides a site prepared and ready for a gravity survey.

Conducting a gravity survey on a longitudinal profile presents complications not addressed here, but if such work were accomplished, then potentially rich and reliable data would result. A network of several intersecting 2-D gravity surveys has the potential to yield a 3-D approximation of the valley floor. Additionally, intersecting surveys would place constraints on the interpretation of the data, leading to inversion that is more reliable. I believe that future gravity investigation on the Juneau Icefield would be practical and beneficial, and I hope that I have been able to supply a beginning framework for such efforts.

WORKS CITED

Benedict, R. J., 1984, Gravity survey on Matthes Glacier, Junueau Icefield, Alaska: Foundation for Glacial and Environmental Research/Juneau Icefield Research Program.

Bull, C., and Hardy, J. R., 1956, The determination of the thickness of a glacier from measurements of the value of gravity: Journal of Glaciology, v. 2, p. 755-762.

Dobrin, M. B., and Savit, C. H., 1988, Introduction to Geophysical Prospecting: New York, McGraw-Hill Book Company.

Hammer, S., 1939, Terrain corrections for gravimeter stations: Geophysics, v. 4, p. 184-194.

-, 1974, Approximation in gravity interpretation calculations: Geophysics, v. 39, no. 2, p. 205-222.

Heiland, C. A., 1940, Geophysical Exploration: New York, Prentice-Hall, Inc.

Hubbert, M. K., 1948, A line-integral method of computing the gravimeter effects of two-dimensional masses: Geophysics, v. 13, p. 215-225.

Isherwood, W., 2004, Personal communication.

LaFehr, T. R., 1991, Standardization in gravity reduction: Geophysics, v. 56, no. 8, p. 1170-1178.

Larsen, C. F., Motyka, R. J., Freymueller, J. T., Echelmeyer, K. A., and Ivins, E. R., 2004, Rapid uplift of Southern Alaska caused by recent ice loss: Geophysical Journal International, v. 158, no. 3, p. 1118-1133.

Miller, M. M., 2004, Personal communication.

Miller, M. M., Benedict, T. D., Sprenke, K. F., Gilbert, G. E., and Stirling, J. R., 1993, New seismic depth profiles on Taku Glacier - 1993: Glaciological and Arctic Sciences Institute, University of Idaho.

Nolan, M., 1992, A cross section of Taku glacier determined by seismic reflection analysis: Juneau Icefield Research Program.

Nolan, M., Motkya, R. J., Echelmeyer, K., and Trabant, D. C., 1995, Ice-thickness measurements of Taku Glacier, Alaska, U.S.A., and their relevance to its recent behavior: Journal of Glaciology, v. 41, no. 139, p. 541-553.

Nowell, D. A. G., 1999, Gravity terrain corrections - an overview: Journal of Applied Geophysics, v. 42, p. 117-134.

Nye, J. F., 1952, The mechanics of glacier flow: Journal of Glaciology, v. 2, no. 12, p. 82-93.

-, 1965, The flow of a glacier in a channel of rectangular, elliptic or parabolic cross-section: Journal of Glaciology, v. 5, no. 41, p. 661-690.

Poulter, T. C., Allen, C. F., and Miller, S. W., 1949, Seismic measurements on the Taku Glacier: Stanford Research Institute.

Russell, R. D., Jacobs, J. A., and Grant, F. S., 1960, Gravity measurements on the Salmon Glacier and adjoining snow field, British Columbia, Canada: Bulletin of the Geological Society of America, v. 71, p. 1223-1230.

Sprenke, K., 2004, Personal communication.

Sprenke, K., Miller, M. M., and J.I.R.P, 1994, Reflection survey of Profile IV, Taku Glacier, Alaska (unpublished data), Foundation for Glacial and Environmental Research/Juneau Icefield Research Program.

Thiel, E., LaChapelle, E., and Behrendt, J., 1957, The thickness of the Lemon Creek Glacier, Alaska, as determined by gravity measurements: Transactions, American Geophysical Union, v. 38, no. 5, p. 745-749.

Venteris, E., and Miller, M. M., 1993, Gravitational profiles on the Taku Glacier system: Foundation for Glacial and Environmental Research/Juneau Icefield Research Program.

APPENDICES

I. Notes on equations used for modeling

Some potential complications arise in applying Equation (3), which was intended for buried bodies, to bodies that lie at the surface. If the glacial surface is not flat, then the tops of some columns will be above the reference plane of some observing stations. On the Taku, the western side of the glacier is 20 m higher than the eastern side, so when calculating the effect of high western columns on low eastern stations, the tops of the columns will be above the elevation of the stations. The positive *z*-direction is defined to be down, so the quantity *d* in (3) will be negative. A negative *d* will change the sign of the tangent in (3), but the negative *d* coefficient will cancel this effect, giving the same result to the equation as if *d* was positive. Thus, mathematically, the effect of a block that extends a distance $|d|$ above the plane of the observing station will have the same gravitational effect as a block whose top truncates a distance $|d|$ below the plane of the observing station. This agrees with the physics, since a mass above the plane of the observing station exerts an upward gravitational force that cancels the effect of a corresponding mass below the plane of the observing station.

Hammer (1974) gives Equation (3) in a slightly different form, and derives the following approximation:

$$\Delta g' = G\delta T \ln\{(u^2 + D^2)/(u^2 + C^2)\} \qquad (12)$$

where $u = x/Z$

$C = 1 - H / 2Z$

$D = 1 + H / 2Z$

T is the width of the block

H is the height of the block

Z is the depth from the station to the center of the block

x is the horizontal distance from the station to the center of the block

This approximation could be used for simplified computations, but it introduces some error, and is unnecessary where computers allow for easy calculation of the exact formula.

II. Modeling Code

The modeling scheme used in this thesis consisted of three major components, all written as m-files for MATLAB 7. The first, "set_up_model.m," creates MATLAB variables for the geometry of the glacier, the locations and elevations of the observing stations, and the locations, elevations, and width of the columns that model the glacier. These variables are used in subsequent m-files. The second, "find_anomaly.m," uses the geometry specified and an assumed thickness of each glacial column to calculate the gravity anomaly at each observing station. The third, "monte_carlo.m," generates random variations to an array of depths and uses find_anomaly.m to calculate the anomalies that each generates. If the anomalies generated by a given array fall within the uncertainty bounds of the relative Bouger anomaly, it keeps the array. It also calculates the roughness of each array, and sorts the arrays from roughest to smoothest.

```
%*************************************************************************
% "Set up model"
% Warren Caldwell (Princeton University '05)
% First in a sequence of m-files used for determining the ice thickness
% of a valley glacier given a Bouger gravity anomaly.
% (Dec 2004 - Apr 2005)
%
% THIS M-FILE IS THE FIRST HALF OF A FORWARD MODEL OF THE GRAVITATIONAL EFFECTS
% OF A VALLEY GLACIER.  REQUIRED USER-DEFINED INPUT DATA ARE AS FOLLOWS:
%
% 1. stat_pos_real.txt must be a text file containing an Nx1 array of the x-locations in meters of
%   N gravity observing stations in the chosen reference frame.  This file must be in the current
%   working directory.
% 2. stat_elev.txt must be a text file containing an Nx1 array of the elevations above sea level in
%   meters of N gravity observing stations.  This file must be in the current working directory.
% 3. glac_start and glac_end are the x-locations of the edges of the glacier in the chosen
%    reference frame.
% 4. anomaly_lowhigh.txt must be a text file containing an Nx2 array where the first column is
%   the lower bound on the Bouger anomaly and the second column is the upper bound.
% 5. rho_ice and rho_rock are the densities of ice and bedrock in kg/m^3.
% 6. The elevations of the model column tops are found by interpolating the elevations of the
%   observing stations.  If any columns tops fall outside the span of the observing stations,
%   MATLAB cannot find their elevations and these must be manually entered into col_elev.
%*************************************************************************

load stat_pos_real.txt;
        stat_pos_real = stat_pos_real';
load stat_elev.txt;
        stat_elev = stat_elev';

glac_start = 50;                        % near edge of glacier
glac_end = 5450;                        % far edge of glacier

load anomaly_lowhigh.txt;
anomaly_obs = mean(anomaly_lowhigh, 2)';
anomaly_low = anomaly_lowhigh(:,1)';
anomaly_high = anomaly_lowhigh(:,2)';
da = (anomaly_high - anomaly_low)/2;  % determines the uncertainty in the observed anomaly.

rho_ice = 900;                          % ice density
rho_rock = 2720;                        % bedrock density



                % Set up columnar model:
col_width = (glac_end - glac_start)/numel(stat_pos_real);
col_pos = linspace(glac_start+(col_width/2), glac_end-(col_width/2), numel(stat_pos_real));
        % col_pos gives the x-location of the center of each column in the model
col_elev = interp1(stat_pos_real, stat_elev, col_pos);

col_elev(16:17) = [1140 1141];    % manually fill in elevations that aren't found by interpolation
```

```
%*******************************************************************************
% "Find anomaly"
% Warren Caldwell (Princeton University '05)
% Second in a sequence of m-files used for determining the ice thickness
% of a valley glacier given a Bouger gravity anomaly.
% (Dec 2004 - Apr 2005)
%
% THIS M-FILE IS THE SECOND HALF OF A FORWARD MODEL OF THE
% GRAVITATIONAL EFFECTS OF A VALLEY GLACIER.
% REQUIRED USER-DEFINED INPUT DATA ARE AS FOLLOWS:
%
% 1. z must be a 1xN array of the ice thickness of each column of
%   the model glacier.  N is both the number of observing stations
%   and the number of columns in the model.
% 2. base_pos is the x-location and base_elev is the elevation of the
%   reference station, used to correct the calculated anomaly for
%   the effect of the anomaly at the reference station.
% 3. The m-file heiland_eq.m is called during this m-file and must
%   be in the current working directory.
%
% Output is "gH," a 1xN array of the anomaly calculated at the
% location of each observing station.
%
%*******************************************************************************

base_pos = 0;
base_elev = 1189.74;

for i = 1 : numel(stat_pos_real);
   gH(i) = 0;
   for j = 1 : numel(col_pos);
      heiland_eq                    % runs subroutine heiland_eq.m
   end
end

% Calculate effect of glacial anomaly on base station.  Use this to correct calculated anomaly.

i = numel(stat_pos_real)+1;
gH(i) = 0;
stat_pos_real(i) = base_pos;
stat_elev(i) = base_elev;
for j = 1 : numel(col_pos);
   heiland_eq                    % runs subroutine heiland_eq.m
end
base_anomaly = gH(i);
gH(i) = [];
stat_pos_real(i) = [];
stat_elev(i) = [];
gH = gH - base_anomaly
```

```
%*************************************************************************
% "heiland eq"
% subroutine for find_anomaly.m
% Warren Caldwell (Princeton University '05)
% 4 November 2004 - April 2005
%
% THIS FILE MUST BE CONTAINED IN THE SAME DIRECTORY AS FIND_ANOMALY.M
%
% Uses equation from Heiland (1940) for the gravitational attraction
%   of a vertical block that is infinite in the y-direction.
%
*************************************************************************

% i is the current observing station and j is the current column, as dictated by the for-loops
%   in find_anomaly.m


d = (stat_elev(i) - col_elev(j));
D = z(j)+d;
xnear = abs(col_pos(j) - stat_pos_real(i)) - (col_width/2);
xfar = abs(col_pos(j) - stat_pos_real(i)) + (col_width/2);

gH(i)=gH(i) + 10^5 * 2 * 6.67e-11*(rho_rock-rho_ice)*...
   (xfar*log(sqrt((D^2+xfar^2)/(d^2+xfar^2)))...
   - xnear*log(sqrt((D^2+xnear^2)/(d^2+xnear^2)))...
   + D*(atan(xfar/D)-atan(xnear/D))...
   - d*(atan2(xfar,d)-atan2(xnear,d)));
```

```
%*************************************************************************
% "Monte Carlo"
% Warren Caldwell (Princeton University '05)
% Third in a sequence of m-files used for finding the ice thickness
% of a valley glacier given a Bouger gravity anomaly.
% (March 2005)
%
% THIS M-FILE GENERATES RANDOM VARIATIONS OF AN INITAL ARRAY OF DEPTHS AND
% KEEPS THOSE FOR WHICH THE GRAVITY ANOMALY GENERATED FALLS WITHIN THE ERROR
% BOUNDS OF THE BOUGER ANOMALY.
% REQUIRED USER-DEFINED INPUT DATA ARE AS FOLLOWS:
%
% 1. z0 must be a 1xN array of depths that serve as the starting point for each variation.
% 2. stop_time is the number of seconds the model will run for.
% 3. stddev is the standard deviation of the normal distribution used for the variation.
%
% Output is zfits, a K x N matrix of K depth arrays, sorted from smoothest to roughest.
% zfits is also saved as a file, zfits1.MAT, in the current directory
%*************************************************************************

stop_time = 3600;                                   % in seconds
stddev = 0.4;                                       % standard deviation

zfits = [];         % Include this command to start a new list or exclude it to continue an old one.
num_fits = size(zfits,1);                           % number of fits thus far
runs = 0;

tic                                                 % begins timing
current_time = toc;
while current_time < stop_time
   runs = runs + 1;
   current_time = toc;

   mfactor = 1 + stddev * randn(size(z0));          % random multiplication factor
   z = z0 .* mfactor;                               % generates a random variation

   find_anomaly % runs find_anomaly.m to calculate gH

   if (gH > anomaly_low) & (gH < anomaly_high)      % tests fit with data of current array
      num_fits = num_fits + 1;
      zfits(num_fits,:) = z;
   end
end
run_time = toc                                      % displays how long the program ran
runs                                        % displays how many variations were tested
num_fits                                            % displays how many were successful
```

% (Continued on following page)

```
                        % Roughness of each z array:
rough=[];
num_fits = size(zfits,1);
for i = 1 : num_fits
   for j = 1 : size(zfits, 2)-1
      rgh(j) = abs(zfits(i,j+1)-zfits(i,j));
   end
   rough(i,1) = sum(rgh);              % measure of the roughness of each z array
end

% Rank the list of z arrays by ascending roughness:
rc = size(zfits,2)+1;                  % column to which roughnesses will be assigned
zfits(:, rc) = rough;                  % place roughnesses into zfits
zfits = sortrows(zfits, rc);           % sort by roughness
rough = zfits(:, rc);                  % obtain sorted roughnesses
zfits(:,rc) = [];                      % clear roughnesses from array of z values.

save('zfits1', 'zfits')                % saves list of arrays as zfits1.MAT
```